Journal Pre-proofs

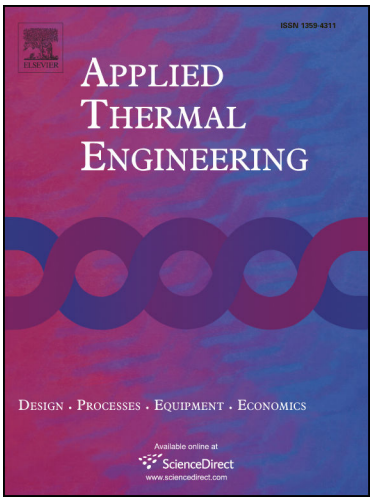

Research Paper

CO_2/acetone mixture desorption process in a plate heat exchanger for compression/resorption heat pumps

Paúl Dávila, Mahmoud Bourouis, Juan Francisco Nicolalde, Javier Martínez-Gómez

PII: S1359-4311(24)00372-7
DOI: https://doi.org/10.1016/j.applthermaleng.2024.122704
Reference: ATE 122704

To appear in: *Applied Thermal Engineering*

Received Date: 27 October 2023
Revised Date: 15 January 2024
Accepted Date: 11 February 2024

Please cite this article as: P. Dávila, M. Bourouis, J. Francisco Nicolalde, J. Martínez-Gómez, CO_2/acetone mixture desorption process in a plate heat exchanger for compression/resorption heat pumps, *Applied Thermal Engineering* (2024), doi: https://doi.org/10.1016/j.applthermaleng.2024.122704

CO_2/acetone mixture desorption process in a plate heat exchanger for compression/resorption heat pumps

Paúl Dávila[12], Mahmoud Bourouis[2], Juan Francisco Nicolalde[134*], Javier Martínez-Gómez[34]

1 Facultad de Ciencias Técnicas, Universidad Internacional Del Ecuador UIDE, Quito 170411, Ecuador.
padavilaal@uide.edu.ec (P.D), junicolaldego@uide.edu.ec (J-F.N)
[2] Departamento de Ingeniería Mecánica, Universitat Rovira i Virgili, Tarragona 43007, España.
mahmoud.bourouis@urv.cat (M.B)
[3]Universidad de Alcalá, Departamento de teoría de la señal y comunicación, (Área de Ingeniería Mecánica) Escuela Politécnica, 28805 Alcalá de Henares, Madrid, España
javier.martinezgomez@uah.es
[4]Facultad de Ingeniería y Ciencias Aplicadas, Universidad Internacional SEK, Albert Einstein s/n and 5th, Quito 170302, Ecuador.
Corresponding:
junicolaldego@uide.edu.ec
Quito -170411, Ecuador.

Highlights

- Modelling of a CRHP with a acetone/CO_2 mixture
- Application of Peng-Robinson equation for zeotropic mixture
- Thermal equilibria calculations for pressure, temperature, and fluid concentration
- Analysis of the coefficient of performance for industrial conditions

Abstract:

Industrial processes represent one of the activities that consume the most energy, which is related to the use of fossil fuels and growing environmental problems. In this way, the recovery of residual heat energy has been presented as an efficient solution to take advantage of low-quality residual heat, where the compressor-resorption heat pump technology has proven to reach high temperature levels with a considerable Coefficient of Performance. The importance of this work lies in the validation of the ecofriendly CO_2/Acetone mixture as a useful working fluid for a compressor-resorption heat pump, initiating the experimental study in the desorption process as a novel application. Even more, the cycle of the bomb has been simulated on previous research regarding a literature comparative and the present work validates it by experimental means. The process of desorption of the CO_2/acetone mixture was studied in a heat exchanger of plates with operating conditions for conducts formed by 4 plates/3 channels, for compression/resorption heat pumps. Result ranges have been obtained for solution heat transfer coefficient between 0.10 to 0.50 $kW \times m^{-2}K^{-1}$, average vapor flow rate between 0.02 and 0.16, heat flow rate between 1.50 to 5.20 $kW \times m^{-2}K^{-1}$ and desorption mass flow rate between 2 to 5 $kg \times m^{-2}s^{-1}$ $x10^{-3}$ in the central channel of the plate heat exchanger. Finally, an empirical correlation is proposed to extend the results of the heat transfer coefficient of the CO_2/acetone solution in applications outside the

experimentally determined range, from the comparison between experimental data and determined by correlation of enthalpy of the solution, an average minimum, mean and maximum deviation of 0.2, 13.5 and 22.3%, respectively, was determined. In this way, the results shows that the most influential variables are the test pressure and heating water temperature at the inlet of the desorber, where, with a concentration of CO_2 (X_{CO2}) between 22 and 25%, the heat transfer coefficients obtained have an order of 0.50 $kW \times m^{-2}K^{-1}$. On the other hand, viscosity favours heat transfer, thermal conductivity is a determining factor for the desorption process. This contributes to lower heat transfer coefficient and heat flow in the heat exchanger for the CO_2/acetone mixture compared to the other mixtures.

Keywords: Heat pump; compression; resorption; desorption process; zeotropic mixture; heat transfer

Nomenclature:

Subscripts

Bo –	Boiling number.
F_{fl} –	Characteristic friction of the fluid.
h_s –	Coefficient of heat transfer of the solution
ρ -	Density
q" –	Heat flow in the exchanger
Co –	Convective number
h_{NC} –	Heat transfer efficiency with combined boiling effect
h_{CD} –	Heat transfer efficiency with dominant convective boiling effect
h_{ND} –	Heat transfer efficiency with dominant nucleated boiling effect
s_{plate} –	Distance between plates
μ –	Dynamic viscosity of the thermal fluid
μ_{amb}–	Dynamic viscosity of the thermal fluid at room temperature
h_{in_s} –	Enthalpy of solution calculated at the inlet of the desorber.
h_{out_s} –	Enthalpy of solution calculated at the outlet of the desorber.
U_G-	Global experimental heat transfer coefficient
X_{CO2G}–	Global mass fraction of CO_2 in the mixture.
T_{int_w} –	Heating water intermediate temperature defined.
T_{in_w} –	Heating water temperature at the exchanger inlet
T_{out_w} –	Heating water temperature at the exchanger outlet
T_{source} –	Heating water temperature at the inlet of the desorber
$LMTD_{des}$ –	LMTD from saturation to boiling of the solution
$LMTD_{sens}$ –	LMTD from subcooling to solution saturation
$LMTD$–	Logarithmic average temperature difference
$\dot{m}_w$ –	Mass flow of heating water
$\dot{m}_s$–	Mass flow of solution

X_{CO2} –	Mass fractionation of CO_2	T_{sub} –	Temperature from subcooling
X_{CO2l} –	Mass fractionation of CO_2 in the liquid phase of the mixture	P_{test} -	Testing Pressure
		q –	Vapour quality of the mixture
Y_{CO2v}–	Mass fraction of CO_2 in the vapour phase of the mixture	V -	Velocity
A_{transf}–	Nominal heat transfer area	μ –	Viscosity
N_c –	Number of solution channels		
β –	Plate angle of the exchanger	*Units*	
e –	Plate thickness	***Area*** -	m^2
a –	Plate width	***Density*** –	kg ×m^{-3}
k_{transf}–	Plate thermal conductivity	***Enthalpy*** -	kJ×kg^{-1}
Pr –	Prandtl number	***Heat Flow*** -	kW ×m^{-2}
Re –	Reynolds number	***Heat Transfer***-	kW×m^{-2}×K^{-1}
Cp_w –	Specific heat of heating water.	***Mass Flow*** -	kg × s^{-1}
h_{LG} –	Specific vaporization enthalpy	***Pressure*** -	Bar
T_{out} –	Temperature at the exchanger	***Specific Heat*** -	kJ×kg^{-1}×K^{-1}
T_{sat}–	Temperature in saturation phase	***Temperature*** -	˚C

1 Introduction

The global demand of energy for heating purposes has been found to be critical in the industry, representing nearly a fifth of the global energy consumption, which is satisfied by using fossil fuels that produces large amounts of carbon emissions[1]. In this way, it is estimated that the demand for heat in industries and buildings has over 75% of the final energy use [2], where, nearly 50% of the industrial energy is lost as waste heat [3]. In this sense, these can be considered as low grade waste heat, defined as a maximum of 100°C [4].

Likewise, heat pump technology allows the thermal revaluation of heat, up to temperatures useful in industrial processes [5], but is limited by the thermodynamic behaviour of working fluids and the resistance of their components. In an open literature review, the research has led to Arpagaus et al. [6] who has conducted a complete and rigorous review on high-temperature compression heat pump technology, that considered more than 20 industrial equipment from 13 different manufacturers, capable of providing heat at a temperature between 90ºC and 165ºC [6]. Ahrens et al [7], highlights that the research activities have been carried out to take advantage of the heat recovery potential of heat pump cycles at a heat supply temperature above 90ºC, and the ongoing research aims to increase the delivery temperatures, regarding the potential above 150ºC that the industry can provide.

Considering its nature of reabsorbing a fluid, the resorption systems are considered alternatives technologies that allows to manage high storage capacity and high heat [8], while in the desorption process the fluid is released. In this way, compression/resorption heat pump technology is an interesting alternative for the thermal revaluation of low-temperature heat, since is the product of the combination of vapor compression and absorption technology, taking advantage the best features of both. Hence, working with two media on a controlled pressure and considering the concentration of the solution, can provide an infinite quantity of temperatures for resorption or desorption [9]. In this sense, this type of heat pump uses a two-component working fluid (refrigerant/absorbent), and its operation is based on the difference in the boiling point of each component to achieve an increase in the temperature of the heat delivered[10].

Furthermore, the European community banned the refrigerants with high Global Warming Potential (GWP) since 2014 [11]. Taking into account this consideration, a conventional fluid used in industrial heat pumps is ammonia, that combined with water is an environmentally friendly refrigerant [12]. In this way, mixtures such as ammonia-water and lithium bromide - water has been used in traditional commercial refrigeration plants [13][14], also $LiNO_3$ (Lithium Nitrate)-ammonia, NaSCN (Sodium Thiocyanate)-ammonia has been studied on absorption heat pumps, however, the ammonia has the drawn back of toxicity [15].

Under this preamble, new working pairs are being sought that are environmentally friendly and exhibit similar or better properties for applications in refrigeration and heat pump systems. In this way, CO_2 is presented as a potential refrigerant substitute to conventional ones, due to its characteristics of no ozone depletion, negligible direct GWP [16], natural refrigerant, non-toxicity, non-flammable, chemically inactive, commercial availability, and that can be combined with absorbent fluids for use in heat pump and cooling cycles. In this sense, due to its low critical temperature (31ºC) and high working pressure, CO_2 has been commonly used in refrigeration applications [17], and considered for binary mixtures with organic solvents [18]. On the other hand, acetone is a solvent with a boiling and fusion temperature of 56.2°C and -95.4°C respectably, it has a solubility on the water of 0.791 $kg \times l^{-1}$ and vapour pressure of 180 mmHg at 20°C [19]

Other authors have investigated this working pair, Groll & Kruse, in 1992, studied the operation of a compression/resorption cooling equipment using the CO_2/acetone mixture with wet compression in vehicle air conditioning applications to replacement of R134a in conventional compression systems [20]. Likewise, in 2000 two patents were published by Spauschus & Hesse, [21] on mixing 200 tubes of CO_2 with different absorbent as co-fluids and the use of scroll compressors (below 35 bar) in the wet compression process. In this sense, understanding the behaviour of the mixtures in different conditions allows to identify possible encounter problems, safe concentration limits and designing efficient and safe process [22]. Mozurkewich et al. [17] used numerical simulation to study the performance of a compression/resorption cycle with wet compression and compare the operation of the cycle with CO_2/acetone and other CO_2 mixtures with N-methyl-2-pyrrolidone, neopentylglycol diacetate and g-butyrolactone operating under the same high pressure and temperature conditions as the conventional R134a system in automobiles, concluding that the results with the CO_2/acetone mixture are the best, but it is convenient to replace the acetone for material compatibility reasons. However, the use of ionic acids in mixture with CO_2 is more recent. K. Li et al., [23] developed a novel CO_2 compression-absorption refrigeration system that reduces the operational pressure on the CO_2 of compression in conventional refrigeration systems. Jin et al., [24] made a comparison of the energy performance of heat pump systems using R744 and R410A refrigerants, where the results showed that the

coefficient of performance (*COP)* of a hybrid heat pump compression/absorption system reaches a value of 3.55 [24]. In the same line of research, Zhao et al., [25] published the experimental results of an air conditioning equipment on a test bench, applying a two-stage method for the integration of heat from a transcritical CO_2 energy cycle to a coal gasification process, where the first stage consisted of optimizing the parameters of the heat integration process and the second in the integration of viable heat into a network of heat exchangers. Sun et al., [26] evaluate the performance of a heat pump system that operate with a CO_2-R32 refrigerant, showing an improvement of the coefficient of performance of 23.3% for the heating and 65.2% for cooling, when the CO_2 fraction was 0.6. C. M. Hsieh & Vrabec, [27] published experimental data for the liquid vapor equilibrium of carbon dioxide dissolved in acetone and pentanones in a temperature range between 313.15 and 353 K up to a pressure of 11.8 MPa [27]. Wu et al., [28] reports that acetone has a high carbon dioxide miscibility and comments that this mixture constitutes an alternative for use in compression/resorption heat pump cycle [28]. Likewise, the research of Ramírez-Ramos et al., [29] studied vapour-liquid equilibrium of the mixture CO_2/acetone from experimental data, for working conditions of 10-110 °C with pressures up to 8.7 MPa, and CO_2 fractions of 0.06-0.82, where the exothermic excess of molar enthalpy were located on the region of the CO_2-rich.

Regarding the use of heat plate exchangers in phase change studies, Tao et al., [30] conducted a study on the condensation process of NH_3 in a 3-plate/2-channel heat exchanger, in a pressure range between 6.30 and 9.30 bar, a cooling temperature between 13.4 and 22.6ºC, achieving a cooling thermal load of 6 kW [30]. Jiménez-García & Rivera, [31] performed a parametric study on a single stage absorption cooling system with a late heat exchanger as the main component to operate with an ammonia-water mixture. The compact design of 0.8m^3 demonstrate steady state conditions, an internal cooling power of 2.6kW, evaporation temperature of 19°C and a coefficient of performance of 0.61 [31]. Furthermore, in the NH_3 evaporation research line Huang et al., [32] studied the boiling process of NH_3 and other refrigerants in plate heat exchangers with different inclination angles (28/28º, 28/60º and 60/60º), where they obtained heat transfer coefficient intervals for each refrigerant studied, who worked with a thermal load in the plate heat exchangers up to 7.65 kW. Khan et al., [33] carried out the experimental study of the process of evaporation of NH_3 and pressure losses in a plate heat exchanger with an inclination of 60ºC of its corrugated channels. This research shows a heat transfer coefficient range of NH_3 between 5.20 and 7.10 $kW \times m^{-2}\ K^{-1}$ at a thermal load on the plate heat exchanger between 2 and 3 kW [33]. Sterner & Sunden, [34] investigate the performance of different plate heat exchangers on the evaporation of ammonia where 5 model were studied, regarding some dimensional differences such as the number of channels from 99, 79 and 63, also corrugation angles of 59 and 65°C. In this way, that heat exchanger with the greater angle and the lowest channels achieved a high and more stable performance at low temperature outlet, while a heat exchanger showed to be more suited for ammonia compared to a similar one, since it had an integrated inlet flow distribution [34]. Itard & Machielsen, [35] analyzed the characteristics of heat transfer during the absorption process of H_2O-dissolved NH_3 in plate heat exchangers and developed experimental correlations of the heat transfer coefficient for the compression/resorption heat pump application [35]. Oronel et al., [36] conducted an experimental study on the absorption and boiling processes with mixtures of $NH_3/LiNO_3$ and $NH_3/(LiNO_3+H_2O)$ in a 4-plate/3-channel heat exchanger, where the solution circulates through the central channel while heating water circulates through the adjacent channels, where temperatures of up to 120ºC were reached with a concentration of NH_3 in the binary mixture between 0.50 to 0.54 and in ternary mixture between 0.435 to 0.465, concluding that the mass absorption flow and heat transfer coefficient of the solution achieved with the ternary mixture were up to 1.6 times higher than those of the binary mixture under similar operating conditions [36]. Amaris et al., [37] proposed the mixtures $NH_3/LiNO_3$ and NH_3 $(LiNO_3+H_2O)$ as suitable working pairs for absorption cooling systems driven by low-temperature heat sources (5 and 40ºC, evaporation and condensation, respectively), where the heat exchangers used as an absorber and desorber were L and H type corrugated plate heat exchangers with a plate

angle of 60 and 30º, respectively, proposing the use of water in the absorbent of the ternary mixture to reduce the viscosity of the binary mixture and increasing the affinity between the refrigerant (NH_3) and the absorbent [37]. Táboas et al., [38] conducted an experimental study of a forced boiling process of the NH_3/H_2O mixture in the central channel of a heat exchanger consisting of 4 plates/3 channels, where the experimentation was carried out under the operating conditions of a generator of an NH_3/H_2O absorption equipment and the effect on the coefficient of heat transfer of solution by the mass flow in the exchanger, heat flow, pressure and concentration of the mixture was studied, concluding that the mass flow has a greater influence on the determination of the heat transfer coefficient of the solution, and the heat flow only influences the value of the solution heat transfer coefficient in the area where the tendency of the coefficients stabilizes, but its effect is small compared to the mass flow.

On the other hand, regarding the use of pure CO_2 and its mixture with different absorbents in plate heat exchangers, under subcritical and transcritical conditions, Tao & Infante Ferreira, [39] performed a review of correlations for the determination of the heat transfer coefficient and friction pressure drop in the condensation process of CO_2 and other fluids in plate heat exchangers with an inclination angle between 25.7 and 70º [39]. Even more, the research of Zendehboudi et al., studied the heat transfer performance of CO_2 as a gas cooler, on a three brazed plate heat exchanger, concluding that the increase of CO_2 inlet pressure can produce a reduction on the heat transfer coefficient , but not in regions of high temperature [40]. Rigola et al., [41] performed a numerical analysis along with an experimental comparison regarding a CO_2 transcritical cycle with working conditions of high medium back pressures, showing that the inclusion of an internal heat exchanger has a significant increase on the COP on the refrigerating cycle and it also increases when the environment temperature increases as well [41]. Furthermore some cases has studied the absorption system in a theoretical way considering the pressure drop as neglectable, but in experiments with different working fluid is not the case [42], which is why the importance of study the systems as experimental cases. Pitarch et al., [43] theoretically analyzed the single- and double-stage air-water heat pump cycles with R744 for hot water production up to 80ºC with a thermal jump of 40ºC. Concluding that a single-stage compressor cycle system is the easiest implementation of all heat pump systems and can achieve a *COP* similar to the two-stage one. Hayes et al., [44] investigated CO_2 condensation in plate heat exchangers with a plate angle of 60/60º, 27/60º and 27/27º. This work was carried out in an operating temperature range between -17.8°C and -34.4°C corresponding to CO_2 subcooling conditions, where a thermal load of the plate heat exchangers between 2.5 and 15 kW was obtained[44]. Regarding the use of acetone in heat exchangers, it is mentioned in the work of Sánchez A. et al. [45]. Regarding the solvency property in prolonged exposure in metal tubes, it is noted that no heat transfer problems occur. This concep is supported by the user manual of plate heat extchangers of ASTRALPOOL [46]

Specifically, this work focuses on the desorption process as part of the compression/resorption heat pump cycle that replaces the evaporator and condenser of a mechanical compression cycle with a desorber and a resorber respectively. It also uses a zeotropic mixture, consisting of a mixture of a volatile fluid (refrigerant) and another of lower volatility (absorbent), in the desorber this mixture evaporates partially resulting in a biphasic [35]. This two-phase current is separated at the outlet of the desorber, the steam stream is sucked in by the compressor and compressed to the high pressure of the cycle while the liquid stream is recirculated to the resorber driven by the solution pump. The steam stream and liquid stream are combined in the mixing component, where it is sought that the amount of steam increases in an adiabatic process. The absorption of the steam from the solution from the mixer takes place in the resorber with high temperature heat production. Figure 1 shows a simplified scheme of the compression/resorption heat pump cycle, its main components and a numbering adapted for study.

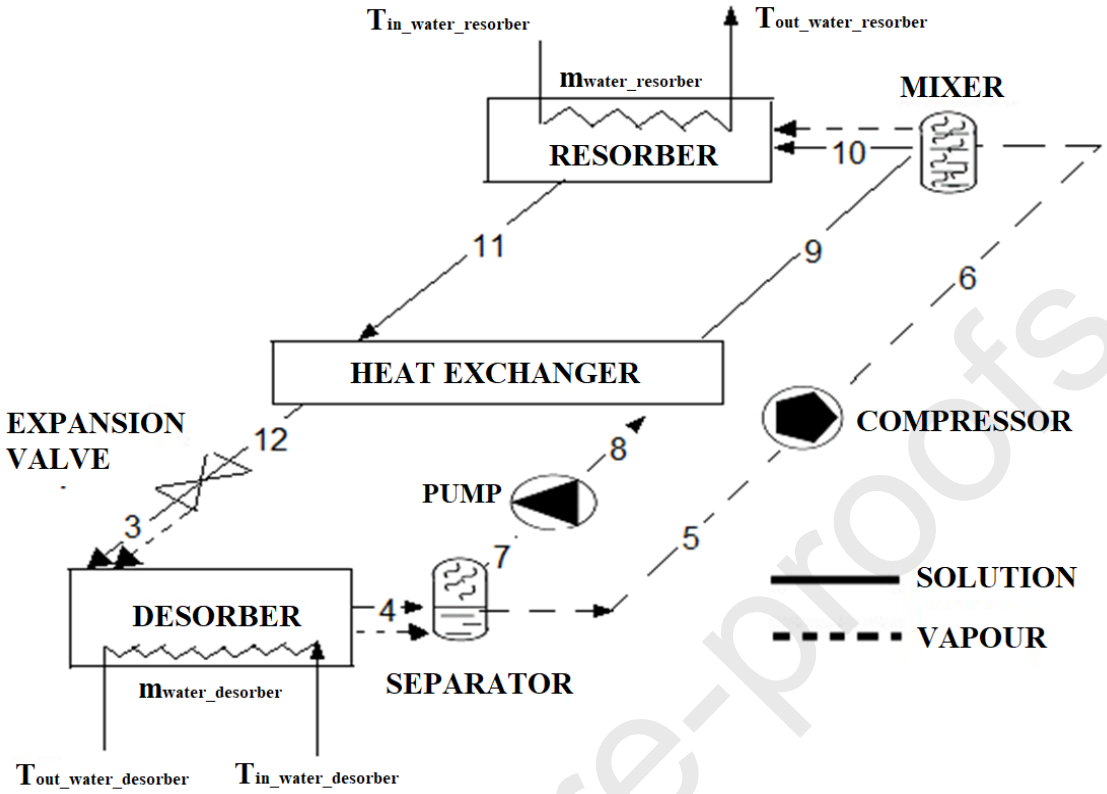

Figure 1. Diagram of the compression/resorption heat pump cycle

The advantages of a compression/resorption heat pump cycle over the conventional steam compression cycle for given conditions in the temperatures of the source and heat supply are: operation of the cycle at lower high pressures, lower compression ratio, reduction of the discharge temperature in the compressor, improved cycle efficiency due to lower internal and external temperature gradients in the resorber and desorbed (Lorentz cycle) and the achievement of higher temperatures in heat production with the use of zeotropic mixtures in comparison to the utilization of pure refrigerants [47][48]. In this sense, the simulation of the heat pump cycle by compression/resorption used the CO_2/acetone mixture was used and the determination of the thermodynamic properties of the mixture, was developed with the Peng Robinson equation of state [49]. The mathematical model developed to perform the simulation of the thermodynamic cycle of compression/resorption was based on the mass and energy balances for each component and the following assumptions: the biphasic mixture is in equilibrium at the input of the desorber and the resorber, it is also assumed state of saturation of the mixture at the output of the desorber and resorber, efficiency of the heat exchanger of the solution equal to 1, compressor and solution pump operate according to isentropic processes with an efficiency also of 1. Furthermore, the resorption/compression cycle model has 5 independent variables: the temperature of the solution at the outlet of the resorber (T_{11}), the temperature of the biphasic current at the outlet of the desorber (T_4), the difference in composition between the overall concentration of CO_2 in the mixture and poor solution ($\Delta x = {}_{global}X - X_{liquid}$), high cycle pressure ($P_{high}$) and mass steam flow ($\dot{m}_v$). In this sense, because of the simulation of the heat pump cycle by compression resorption, the pressure, temperature, and molar concentration intervals of CO_2 dissolved in acetone are defined, in which the cycle operates as a heat pump in table 1[50].

Table 1. Operating intervals of the CRHP cycle using the CO2/acetone mixture [50]

Variable	Interval	Unit
Molar concentration of CO_2	0.20 – 0.50	[-]
High cycle pressure	30 - 50	bar
Temperature of the solution at the outlet of the desorber	30 - 70	˚C
Solution temperature at resorber outlet	50 - 100	˚C

The innovative contribution of this work carries out an experimental study of the desorption process of the CO_2/acetone mixture in a plate heat exchanger, whose results are useful for compression/resorption heat pumps operated with this working mixture. The operating conditions of the experimental equipment will be determined from the simulation of the thermodynamic cycle of heat pump by compression/resorption and the limiting geometric characteristics of the plate heat exchanger used as a desorber. Developing a description of the experimental equipment designed and built for the study of the desorption process of the CO_2/acetone mixture and its set-up, along with a methodology for reducing experimental data obtained in experiences carried out and results of the main parameters of heat and mass transfer, heat transfer coefficient of the solution, average vapour quality, desorption mass flow and heat flow in the exchanger. Finally, an empirical correlation is proposed for the determination of the heat transfer coefficient of the CO_2/acetone solution in a mass fraction range of CO_2 dissolved in acetone, wider than that studied in this work, for compression/resorption heat pump applications. Furthermore, the research of compression-resorption systems has been studied by several authors, considering the variety of applications [51], while the mixture CO_2/Acetone has applications of interest considering that has an operating temperature lower than 200˚C compared to other working fluids [7], what makes it a not very much studied system, granting a novelty component to the present research. This work aims to be a tool to identify the advantages and limitations of the CO_2/acetone work pair in a compression/resorption heat pump cycle, starting its experimental study by the desorption process with support in the determination of the properties of this mixture, already published in a previous article.

2 Method

The method to perform the study of the desorption process of the CO_2/acetone mixture in a plate heat exchanger is described as follows. Specifying the criteria taken for the determination of the independent variables and their operating intervals in the experimental equipment. Likewise, the main circuits and components that constitutes the experimental equipment built are described, along with its set-up process.

2.1 Plate heat exchanger used in the experimental study.

In the present work, the same plate heat exchanger used in the works of Oronel et al., [36] and Táboas et al., [38] will be used. The heat exchanger used for the study of the desorption process has four plates forming three channels; the CO_2/acetone solution circulates through the central channel while the heating water stream circulates through the adjacent channels. Táboas et al., [38] accomplished the desorption process of the NH_3/H_2O mixture up to temperatures of 140°C

and 15 bar pressure in the same plate heat exchanger [38]. In this sense, the data was taken from the area of the cross-section of the solution channel and the maximum and minimum volumetric flows obtained from heat transfer tests with water on both sides of the exchanger at water temperatures between 20ºC and 80ºC, obtaining a value of 0.034 litters× s^{-1} and 0.010 litters×s^{-1} respectively. In this way, table 2 shows the main geometric and operational characteristics of the heat exchanger to be used in the experimental equipment for the study of the desorption of the CO_2/acetone mixture. This plate heat exchanger corresponds to the NB51 model, Alfa Laval, with 30º corrugation of plate inclination with respect to the horizontal, also, figure 2 shows an outline of the main dimensions and information of the inclination and corrugation of the plate of the heat exchanger used as a desorber.

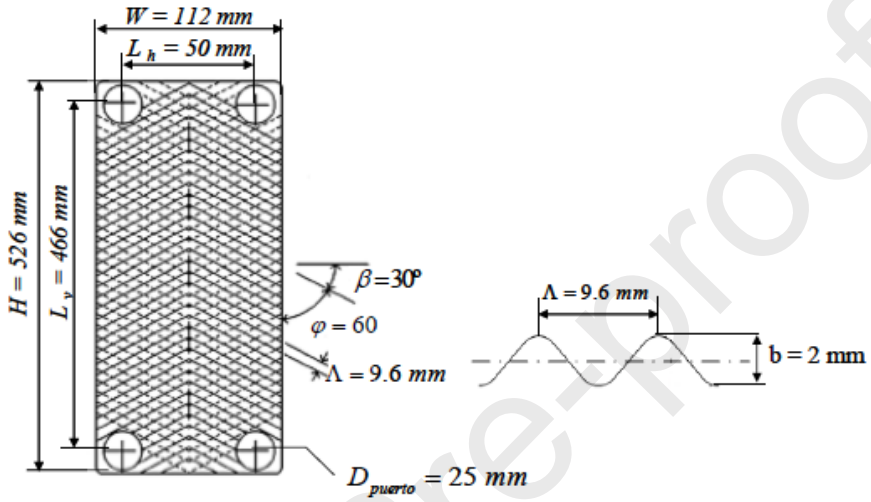

Figure 2. Geometric dimensions of the plate heat exchanger used as a desorber [38]

Table 2. Characteristics of the plate heat exchanger used as a desorber in the experimental study.

Description	Value	Unit
Plate area	0.05	m^2
Heat transfer area (A_{transf})	2	cm^2
Separation between plates	2	mm
Plate thickness (e)	0.4	mm
Hydraulic diameter	0.004	m
Maximum operating pressure	21	bar

2.2 Independent variables and operating intervals

The operating conditions of the desorber and the sizing of the experimental installation have been determined based on two criteria: the pressure, temperature and molar fraction ranges of CO_2 dissolved in acetone determined in the simulation of the compression/resorption heat pump cycle and operating restrictions of the plate heat exchanger used as a desorber. The conditions determined for the operation of the experimental equipment are defined in table 3.

Table 3. Independent variables and operating intervals for the experimental study of the desorption process of the CO_2/acetone mixture

Operation variable	Symbology	Operating interval	Unit
Mass fraction of CO_2 added to absorbent mass (acetone)	X_{CO2}	20 - 30	%
Testing pressure	P_{test}	10 - 18	bar
Heating water temperature at the inlet of the desorber	T_{source}	40 - 60	˚C
Logarithmic average temperature difference of the desorber	*LMTD*	5 - 20	˚C
Mean solution mass flow	$\dot{m}_s$	0.005	$kg \times s^{-1}$

2.3 Description of the experimental facility for the study

The experimental equipment consists of two main circuits: loading or preparation circuit of the mixture (red line) and solution or test circuit (black line), where figure 3 shows a simplified scheme of the experimental device, indicating its components, the different currents that are part of it and the numbering of the different points of the cycle for its study and the corresponding description of the circuits are described as follows.

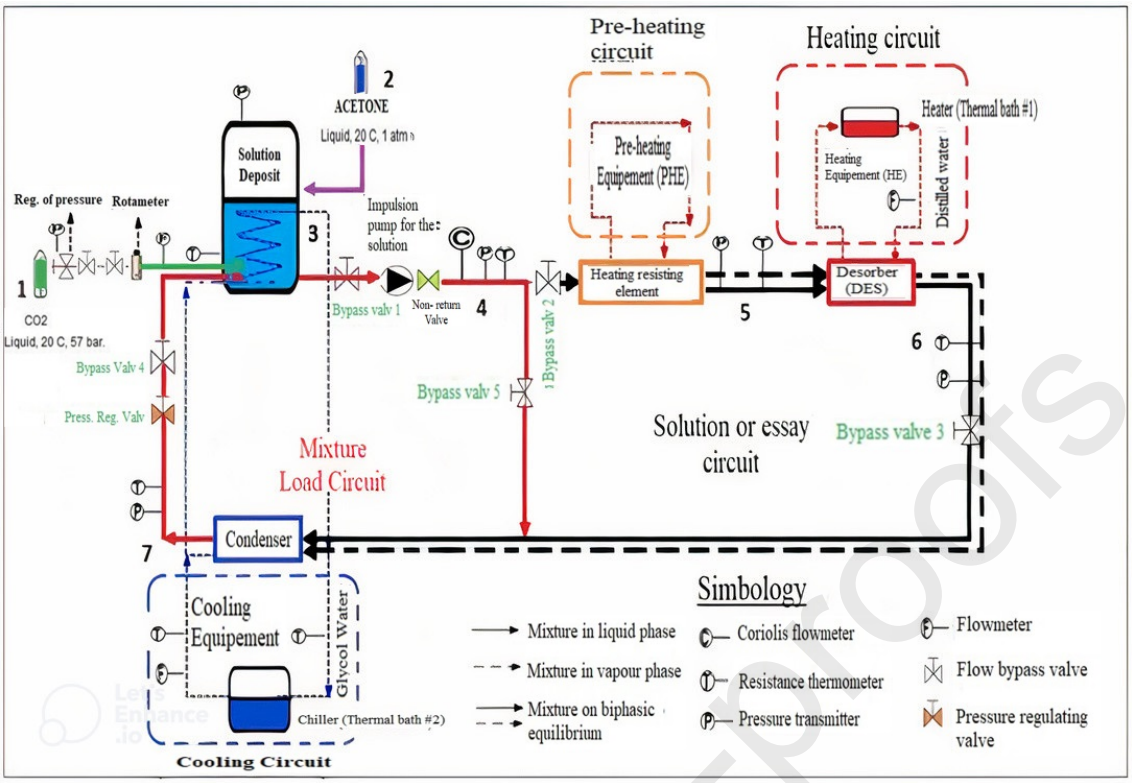

Figure 3. Diagram of the experimental equipment

2.3.1 The loading or preparation circuit of the mixture

The first circuit is composed by a solution tank, the impulsion pump for the solution, a Coriolis type flowmeter, a plate heat exchanger that works as a condenser and a chiller (Thermal bath #2). This circuit corresponds to the circuit where the mixture is prepared at a certain concentration of CO_2 dissolved in acetone. In the tank the pure components are mixed, and the mixture is stabilized at an equilibrium pressure (3), then through the pump (4) the mixture is driven by the circulation pipe (3, 4 and 7) to improve the process of absorption of CO_2 by the acetone. The mass flow is regulated by means of a frequency inverter that regulates the revolutions of the motor connected to the pump. The mixture is directed to the condenser (plate heat exchanger) for condensation and heat dissipation, where the higher the overall concentration of CO_2 in the mixture, lower temperatures are needed for it to be in the liquid phase. Likewise, the temperature of the external fluid (Water – glycol 45%) that pumps the external cooling circuit (thermal bath #2) is controlled. Finally, the mixture returns to the initial tank (3).

2.3.2 The solution or test circuit of the mixture

On the other hand, the second circuit is composed by the solution tank, impulsion pump for the solution, Coriolis type flowmeter, a heating resistive element (electrical resistance), a plate heat exchanger that operates as a desorber, a plate heat exchanger that operates as a condenser, heater (Thermal bath # 1), chiller (Thermal bath # 2) and a pressure regulating valve at the outlet of the condenser for the regulation of the test pressure. In this way, this scheme corresponds to the circuit of analysis of the process of desorption of the mixture that is also made up of two external circuits composed by the heating equipment (HE) that corresponds to the thermal bath #1, that pumps distilled water into the desorber to reheat the CO_2/acetone solution that comes from the pre-

heating equipment (PHE), and the external cooling circuit corresponds to thermal bath #2, where a portion of this cooling flow is directed toward an internal coil in the reservoir and the Coriolis type flowmeter measures the density and flow rate that is passing through the pump to the load line or performing the test.

The description of the instrumentation and control for the experimental study of the desorption process of the CO2/acetone mixture in a plate heat exchanger and the process of loading the CO2/acetone mixture into the experimental apparatus, tuning and determination of the stationary conditions are described in Appendix A and B, respectively.

2.4 Reduction of experimental data

The recording and processing of experimental data in the input and output currents of the CO_2/acetone mixture in the desorber allows to determine the coefficient of heat transfer of solution (h_S), mean vapour quality (q_{med}), heat flow in the heat exchanger (q") and mass flow of desorption of the solution ($\dot{m}_{des}$). In this way, the method of calculating the different heat and mass transfer parameters in the desorption process of the CO_2/acetone mixture is presented as follows, where the thermal load of the desorber is determined by the energy balance on the solution side as shown in equation (1) [51] [10].

$$\dot{Q}_{des} = \dot{m}_s \times (h_{out\_s} - h_{in\_s}) \quad (1)$$

Furthermore, the global experimental heat transfer coefficient (U_G) is determined from the thermal load of the desorber, the logarithmic mean temperature difference (LMTD) and the heat transfer surface area (A_{transf}), as displayed in equation (2) [51] [10].

$$U_G = \frac{\dot{Q}_{des}}{(A_{transf} * LMTD)} \quad (2)$$

In this way, the mixture can enter the exchanger as subcooled saturated or biphasic balance, and if the mixture enters the exchanger in subcooling, the LMTD is defined in two parts: a first from subcooling to saturation of the solution expressed in equation (3) and the second part from saturation point to boiling showed in equation (4) [51] [10]

$$LMTD_{sens} = \frac{(T_{int\_w} - T_{sat\_s}) - }{Ln\left(\frac{T_{int\_w}}{T_{out\_w}}\right.} \quad (3)$$

$$LMTD_{des} = \frac{(T_{in\_w} - T_{out\_s}) - }{Ln\left(\frac{T_{in\_w}}{T_{int\_w}}\right.} \quad (4)$$

Furthermore, the T_{int_a} is defined with equation (5) where Q_{sens} represents the thermal load on the exchanger from subcooling to saturation [51] [10].

$$T_{int\_w} = T_{out\_w} + \left(\frac{\dot{Q}_s}{\dot{m}_w}\right. \quad (5)$$

On the other hand, regarding the mean vapour quality in the exchanger it is considered that if the solution enters the exchanger under conditions of subcooling or saturation the vapour quality is zero. In this way, if the solution enters the exchanger under two-phase equilibrium conditions, the steam quality at the exchanger input is calculated by means of equation (6) [51] [10].

$$q = \frac{X_{CO2\_G} - X_{CO2\_l}}{Y_{CO2\_v} - X_{CO2\_l}} \quad (6)$$

Even more, the same definition of equation (6) is used for the calculation of the mean vapour quality of the mixture at the evaporator, where the mean vapour quality in the desorber is calculated as the arithmetic mean between the vapour quality at the inlet and outlet of the plate heat exchanger, as shown in equation (7) [51] [10].

$$q_{med} = \frac{q_{in} + q_{out}}{2} \quad (7)$$

The calculation of the heat transfer coefficient of the heating water (h_w) used in this work was obtained by the procedure suggested by Táboas et al., consisting in the use of the correlation in simple phase expressed by T. S. Khan et al., [52] where the calculation of the Nusselt number is shown in equation (8), where selection of the constants "C_1" and "m" used in this correlation are required.

$$Nu = C_1.Re^m.Pr^{0.33}(\frac{\mu}{\mu_{an}} \quad (8)$$

In this way, the constants used for the Nusselt number are shown in Table 4, and the plate heat exchanger used as a desorber has a corrugation angle β = 30 °, and the Reynolds number was calculated by means of equation (9) [52], considering V_w as the velocity of the heating water, ρ_w is the density of the heating water and μ_w is the dynamic viscosity of the heating water.

Table 4. Constants for Kumar correlation [37]

B	***Re***	***C_1***	***m***
≤ 30	≤ 10	0.718	0.349
	10 >*Re*< 400	0.348	0.663

$$Re = \frac{V_w.\rho_w.D_H}{\mu_w} \quad (9)$$

On the other hand, the Nusselt number can be calculated from the heat transfer coefficient of the heating water (h_w), as shown in equation (10), being γ_w the thermal conductivity of the heating water and D_H the hydraulic diameter [52].

$$Nu = \frac{h_w . D_H}{\gamma_w} \qquad (10)$$

In this way, if the solution enters the heat exchanger in subcooling, the properties of the heating water must be calculated in two intervals of average temperatures: from subcooling to saturation (T_{sub_w}) and from saturation to boiling of the solution (T_{des_W}). These temperatures are calculated with equations (11) and (12) respectively.

$$T_{sub\_w} = \frac{T_{in\_w} + T_{out\_w}}{2} \qquad (11)$$

$$T_{des\_w} = \frac{T_{int\_w} + T_{in\_w}}{2} \qquad (12)$$

The range of values calculated for the Reynolds and Prandtl numbers in the present paper is shown in Table 5.

Table 5. Interval of calculated values for Reynolds, Prandtl and Nusselt numbers in heating water

Number	Range of values
Reynolds	60 – 380
Prandtl	2.98 – 5.41
Nusselt	8.10 – 20.50

The heat transfer coefficient of the CO_2/acetone solution (h_s) is calculated from the heat transfer coefficient of the heating water (h_w), and the relationship between the overall experimental heat transfer coefficient (U_G) and the geometric characteristics and plate material of the heat exchanger, is expressed on equation (13) [52], considering e the width of the exchanger's plate and k_{transf} its thermal conductivity.

$$\frac{1}{h_S} = \frac{1}{U_G} - \frac{1}{h_a} - \frac{e}{k_{transf}} \quad (13)$$

To calculate the heat transfer coefficient of the solution, it must be determined whether the solution enters the desorber as a subcooled liquid or as a vapor-liquid mixture. In this way, the calculation of the heat transfer coefficient of the solution for a single liquid phase (h_l) in the event that the solution enters the heat exchanger in subcooling is carried out through the procedure proposed in the work of Hsieh Y. & Lin, [53] where the expression for this calculation is expressed in equation (14), that considers Nu_l as the Nusselt number, k_l the thermal conductivity of the solution in liquid phase and D_h the hydraulic diameter [53].

$$h_l = Nu_l \times k_l \times D_h{}^{-1} \quad (14)$$

Cieśliński et al., [54] define in their work "Heat transfer in plate heat exchanger channels: Experimental validation of selected correlation equations" the Nusselt number for the calculation of the transfer coefficient in liquid phase, this correlation is a modification of the Dittus – Boelter equation and is expressed in equations (15) to (18) [54].

$$Nu_l = C(\beta) \left(Re^{0.728+0.0543 \sin\left[\frac{2\pi\beta}{90}\right.} Pr^{\frac{1}{3}} \quad (15)$$

$$C(\beta) = 0.2668 - 0.006 + 7.24 \quad (16)$$

$$Re = \frac{v_c \times D_{H*} \rho_s}{\mu_s} \quad (17)$$

$$v_c = \frac{\dot{m}_s}{a \times s_{plate} \times N_c} \quad (18)$$

Herold et al., [55] define desorption as the partial generation of vapor in a solution, where the concentration of a component is higher, unlike evaporation where it is assumed that all components are fully vaporized [55]. In this way, the desorption mass flow ($\dot{m}_{des}$) is defined as a function of the vapour quality considering q_{out} and q_{in} as the vapour quality of the mixture at the outlet and inlet of the desorber, respectively (19). The value of the desorption flow is conditioned by the vapour quality at the inlet of the heat exchanger, considering that if the solution enters subcooled or saturated this is zero. Furthermore, the heat flow in the desorber (q") is calculated through equation (20) [55].

$$\dot{m}_{des} = \frac{(q_{out} - q_{in}).\dot{m}_s}{A_{plate}} \quad (19)$$

$$q" = \frac{h_{out_s} - h_{in_s}}{A_{plate}} \quad (20)$$

Where: A_{plate} is the plate in the heat exchanger

2.5 Uncertainty Calculation for Determination of Solution Heat Transfer Coefficient (h_S)

The validation of the results obtained requires the calculation uncertainty in the desorption process of the CO_2/Acetone mixture within the central channel of the plate heat exchanger. This determination has considered the parameters that influence it. The order in which the uncertainty of the process is determinate is developed as follows:

1. Uncertainty in the calculation of the concentration of the prepared CO_2/Acetone mixture from density and temperature.
2. Uncertainty in the calculation of enthalpies of the solution at the inlet of the desorber from the enthalpies of pure fluids.
3. Uncertainty in the calculation of working pressure.
4. Uncertainty in the calculation of the enthalpy of formation of the mixture in liquid phase and vapor phase
5. Global enthalpy uncertainty of solution at the desorber input.
6. The same calculation procedure for the overall enthalpy of solution at the outlet of the desorber.
7. Solution mass flow measurement uncertainty.

8. Uncertainty of mixing heat determination on the solution (internal) side of the plate heat exchanger.
9. Solution heat determination uncertainty on the heating (external) side of the plate heat exchanger.
10. Determination of Solution Heat Transfer Coefficient (h_s)

3 Results and discussion

The experimental tests were carried out in an operating pressure range (*Test pressure*) between 10 and 18 bar, at a mass fraction of CO_2 (X_{CO2}) diluted in acetone between 22 and 31%, inlet temperature in the heating water (T_{source}) from 40 to 60ºC, a LMTD between 5 and 20ºC and a mass flow of medium solution of 0.005 kg×s^{-1}. In this way, the results obtained in the experimental facility designed and built to characterize the desorption process of the CO_2/acetone mixture in a plate heat exchanger are shown as follows.

3.1 Heat transfer coefficient of the CO_2/acetone solution

The following results (figures 4 to 6) shows the values of h_s as a function of the test pressure and the inlet temperature of the heating water (*source T*), to mass fractions of CO_2 (X_{CO2}) dissolved in acetone of a) 22% b) 25% c) 28% and d) 31%.

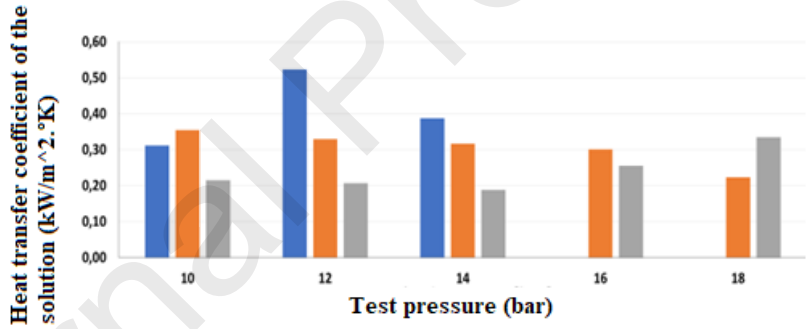

a)

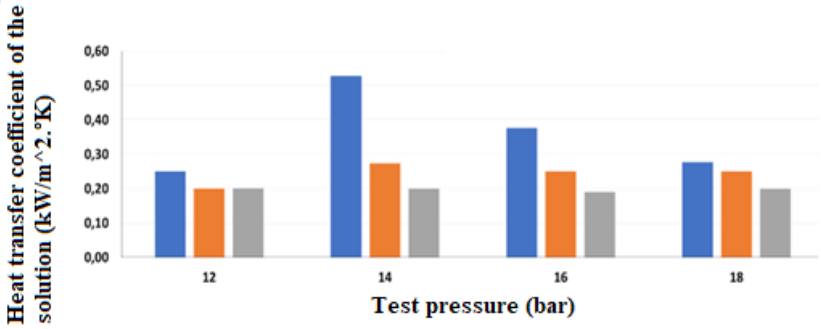

b)

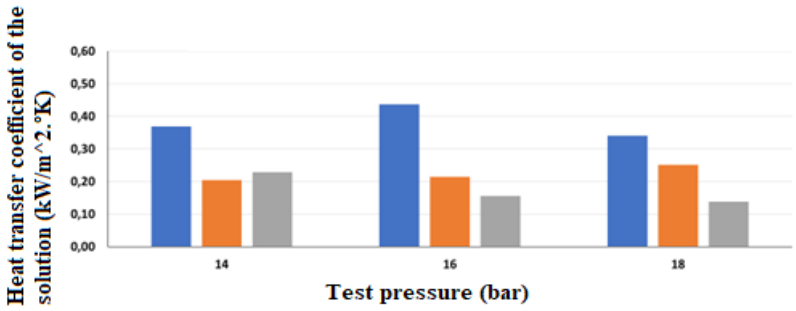

c)

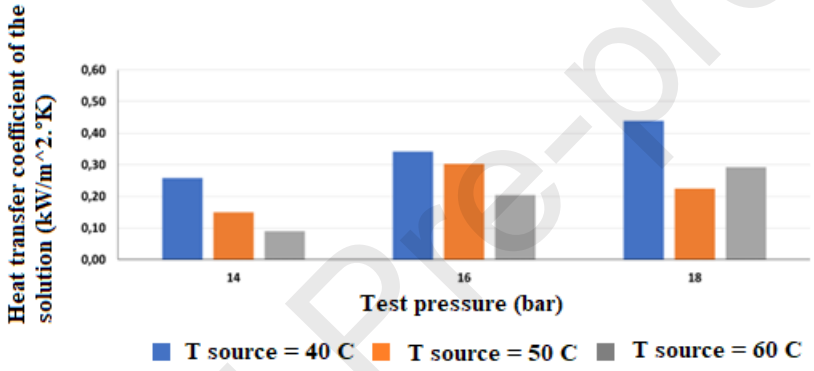

d)

Figure 4. Variation of the heat transfer coefficient (*hs*) LMTD 5 ºC - 12ºC. Mass fractions of CO_2 (X_{CO2}) dissolved in acetone a) 22% b) 25% c) 28% and d) 31%.

Figure 4 shows that the heat transfer coefficient h_s was determined at a heating water temperature at the inlet of the desorber between 40 and 60ºC. If the temperature of the heating water increases from 40 to 60ºC, a decreasing trend is observed in the values of h_s for a test pressure between 10 and 16 bar, for a pressure of 18 bar this trend changes for a mass fraction of 22 and 31%, determining that in these cases the solution enters the desorber in a subcooling state. Even more, if the LMTD is between 5 and 12ºC, the value of the heat transfer coefficient h_s reaches a maximum value defined by the mass fraction of CO_2 in the CO_2/acetone mixture at a test pressure, and then reduces its value to higher pressures.

On the other hand, figure 5 presents the results of the heat transfer coefficient when the LMTD is between 12 and 15ºC, showing that if the test pressure is maintained constant and the temperature in the heating water at the inlet of the desorber is increased by 50 to 60ºC, the values of h_s of grow at an average rate of 30% of the highest value, this to each mass fraction of CO_2 in the CO_2/acetone mixture and a test pressure between 10 and 16 bar, a 18 bar can change this trend. If the test pressure increases from 10 to 16 bar and T_{source} is constant, a trend of increase in h_s is observed,

the highest determined value of h_s is 0.42 kW×m^{-2}K^{-1}. In this way, when the LMTD is between 12 and 15°C, the highest values of h_s were calculated at a test pressure of 16 bar.

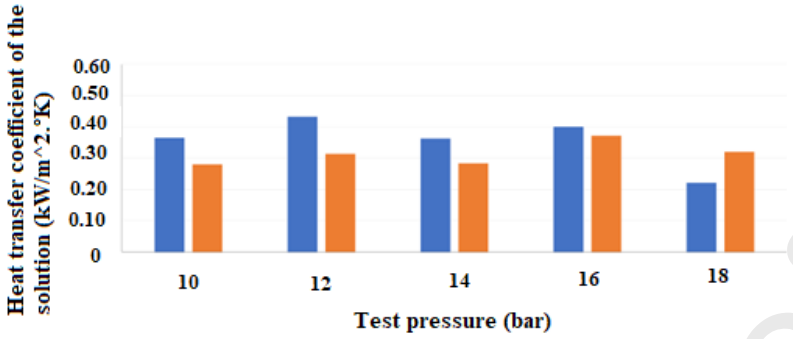

a)

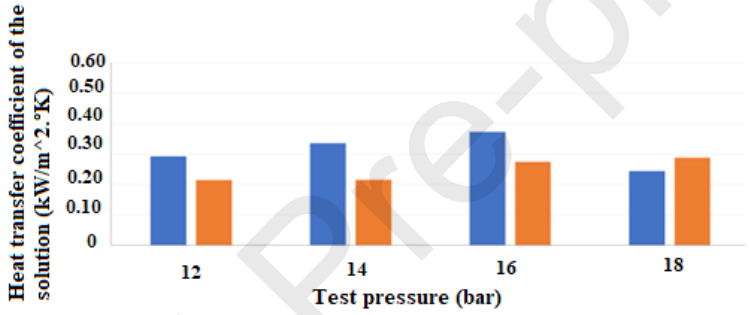

b)

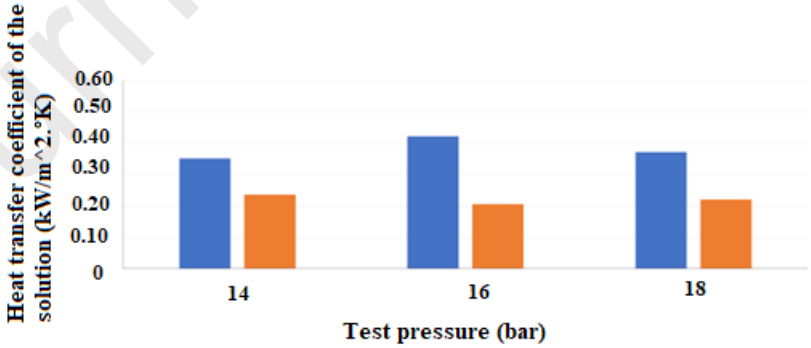

c)

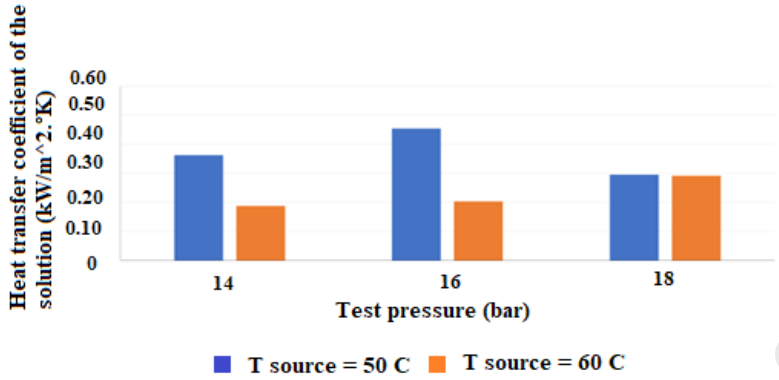

d)

Figure 5. Variation of the heat transfer coefficient (hs) LMTD 12ºC - 15 ºC. Mass fractions of CO_2 (X_{CO2}) dissolved in acetone a) 22% b) 25% c) 28% and d) 31%.

Furthermore, figure 6 corresponds to the results of *hs* at a LMTD between 15 and 20ºC, a mass fraction of a)25% b)28% and c)31% of CO_2 dissolved in acetone and a temperature in the heating water at the inlet of the desorber of 60ºC.

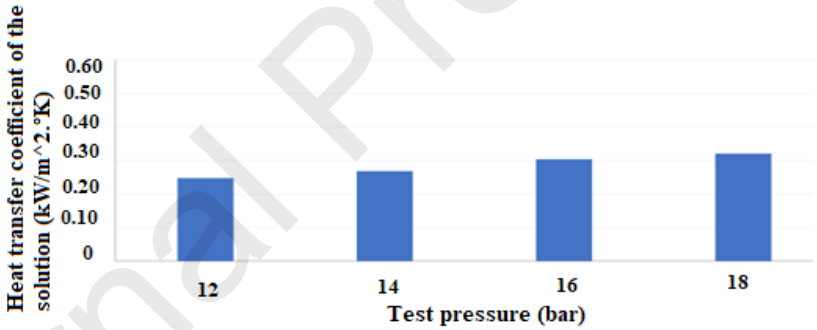

a)

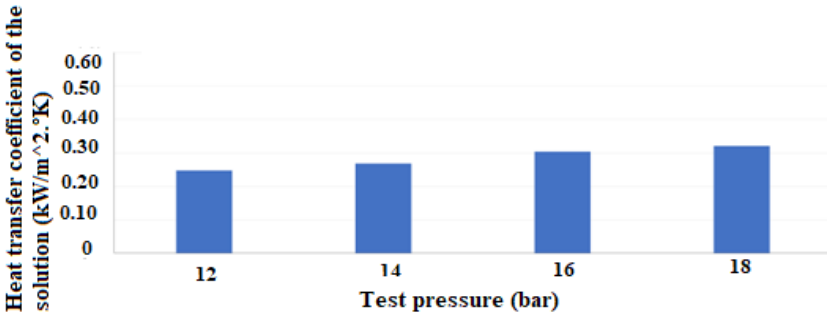

b)

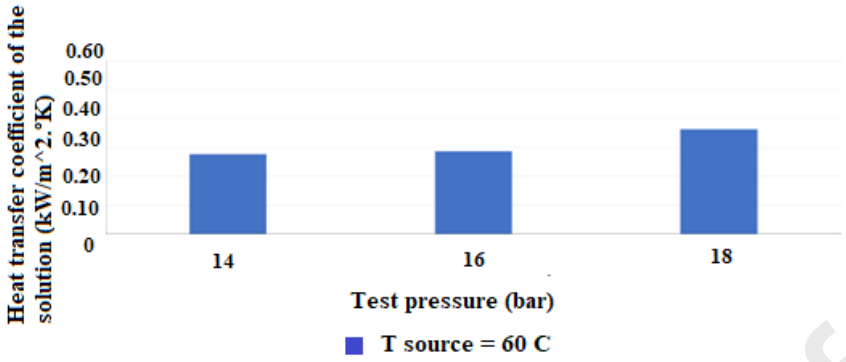

c)

Figure 6. Variation of the heat transfer coefficient (hs) LMTD 15 ºC - 20ºC. Mass fractions of CO_2 (X_{CO2}) dissolved in acetone a) 25% b) 28% and c) 31%.

Figure 6 shows that the highest determined value of h_s is 0.38 $kW \times m^{-2}K^{-1}$, this value is obtained at the test pressure of 18 bar and an X_{CO2} of 31%. In this way, it is observed a growth trend in the value of h_s when the test pressure increases from 12 to 18 bar, where, if the mass fraction of CO_2 in the CO_2/acetone mixture exceeds 25 and 31%, the values of h_s are almost constant if a constant pressure value is taken. Even more, no values of h_s were determined for a mass fraction of 22% or at temperatures of the heat source between 40 and 50ºC, because no valid trials could be recorded.

Overall, the values of h_s meet a tendency of decrease when the test pressure increases from a value of 10 to 16 bar, this trend changes for some cases where the test pressure is 18 bar. If the heating water temperature increases by 40 and 60ºC, a decreasing trend is observed in the values of the heat transfer coefficient (h_s), and even more, if the LMTD increases from 5 to 20ºC and the mass fraction of CO_2 in the CO_2/acetone (X_{CO2}) mixture from 22 to 31%, the values of h_s of increase by an average trend of 15% at each test pressure.

3.2 Mean vapour quality in the desorber.

Figure 7 shows the mean vapour quality between the inlet and outlet of the plate heat exchanger as a function of the test pressure and its respective sub-figures a, b, c, and d correspond to the values determined for a mass fraction of 22, 25, 28 and 31% of CO_2 dissolved in acetone, respectively. Each sub-figure shows the heating water temperature (*source T*) and the LMTD. In this way, the determined value of q_{med} decreases in an average trend of 10% for every 2 bar increase in test pressure between 10 and 18 bar, as the concentration in mass fraction of CO_2 dissolved in acetone increases from 22 to 31%, the mean vapour quality also does so in an average trend of 5%. Furthermore, a high value of the temperature in the hot water at the inlet of the desorber (60ºC) and a logarithmic average temperature difference between 5 and 12ºC, generate the highest mean vapour quality in the desorber, whose value is 0.162. In this way, the minimum value of q_{med} is 0.02, this is determined with a heating water temperature of 40ºC and a test pressure of 18 bar.

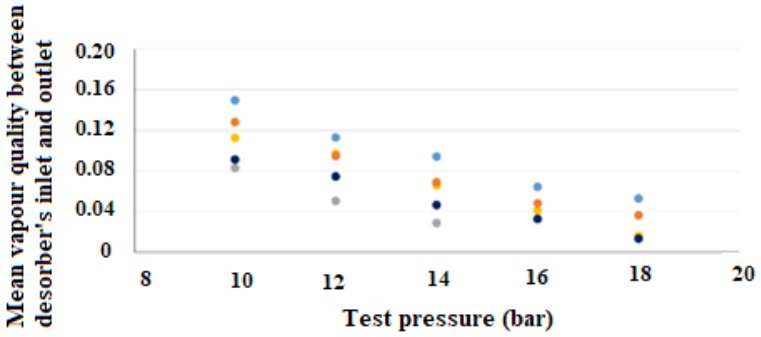

a)

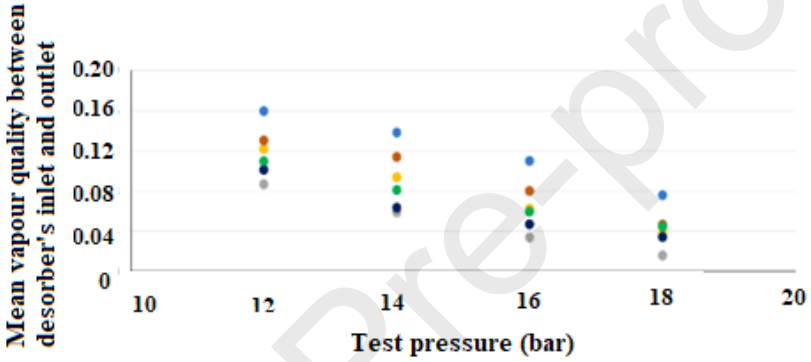

b)

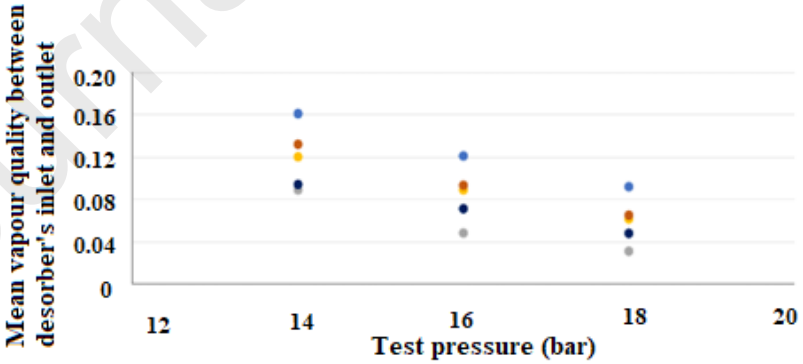

c)

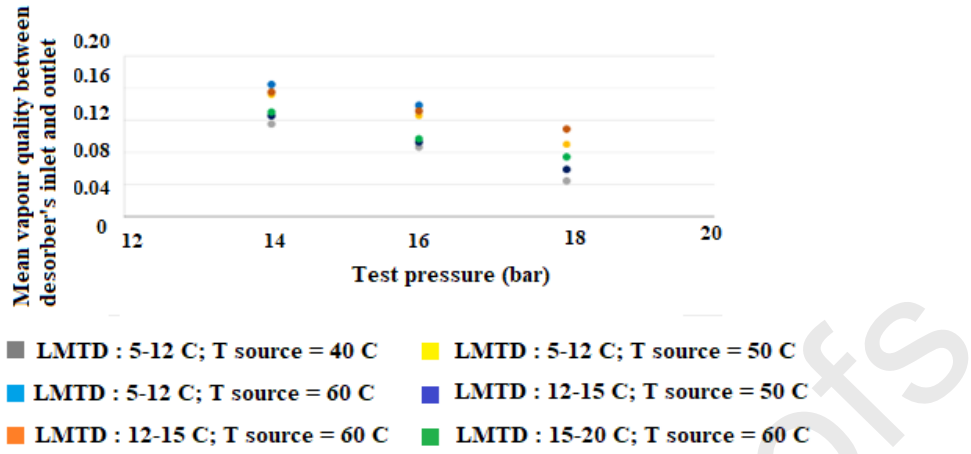

d)

Figure 7. Variation of the mean vapour quality. Mass fractions of CO_2 (X_{CO2}) dissolved in acetone a) 22% b) 25% c) 28% and d) 31%.

3.3 Heat flow in the desorber

The results of figures 8 to 10 show the heat flow values (q") as a function of the independent variables: temperature of the heating water at the desorber inlet (T_{source}), mass fractions of CO_2 (XCO_2) dissolved in acetone from a) 22, b)25, c)28 and d)31%, test pressure (P_{test}) between 10 and 18 bar, and a LMTD in the intervals of: 5 to 12ºC, 12 to 15ºC and 15 at 20°C, respectively.

In this sense, the results of heat flow (q") determined for a LMTD between 5 and 12ºC (Figure 8), show a reduction in heat flow if the temperature of the heating water at the inlet of the desorber (T_{source}) increases from a value of 40 to 60ºC. In this sense, this behaviour is produced if the temperature in the heat source increases, a higher vapour quality is generated in the mixture, but the heat flow decreases. An increasing trend in q'' has been determined that depends on the amount of CO_2 dissolved in the CO_2/acetone mixture when the test pressure increases (10 to 18 bar), up to a maximum value, from this maximum point, there is a decrease of q'' at an average rate of 20% for each increase of 2 bar in the test pressure. The range of q" for a LMTD between 5 and 12ºC was determined between 1.5 and 3.1 $kW \times m^{-2}$.

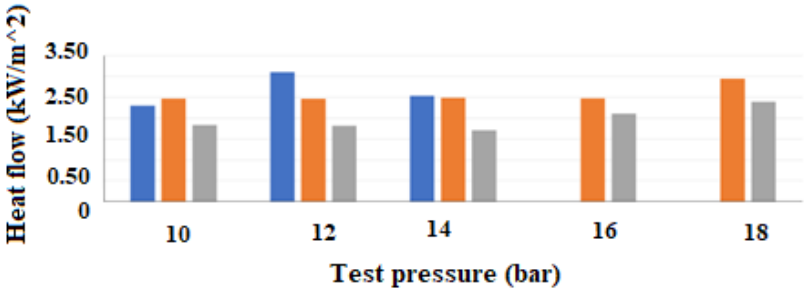

a)

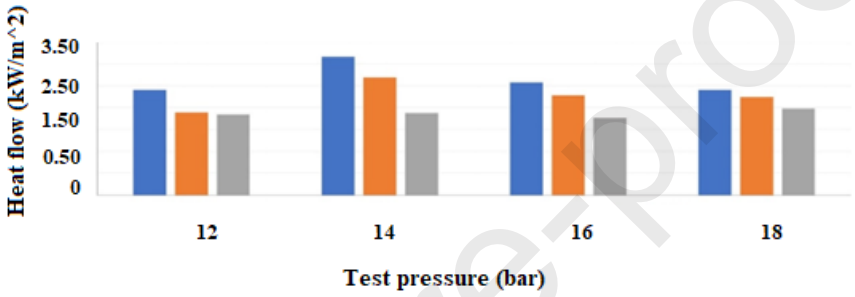

b)

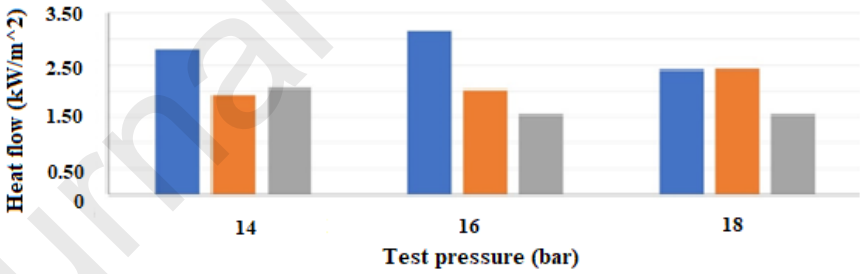

c)

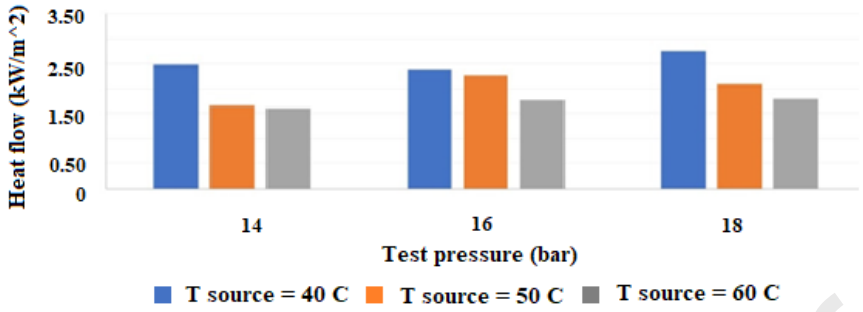

d)

Figure 8. Variation of the heat flow for LMTD 5 to 12 °C. Mass fractions of CO_2 (X_{CO2}) dissolved in acetone a) 22% b) 25% c) 28% and d) 31%.

On the other hand, figure 9 shows a reduction in heat flow with respect to an increase in temperature in the heating water at the desorber of 50 to 60ºC, where the heat flow range obtained in this case is between 1.5 and 5 kW×m^{-2}. This figure shows that for a LMTD between 12 and 15°C, where the highest heat flow values are obtained when the test pressure is between 14 and 16 bar.

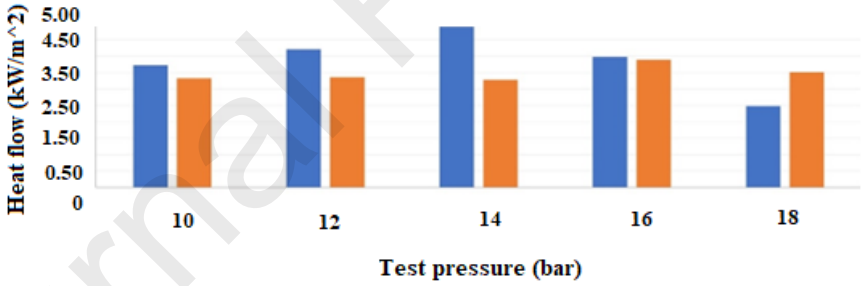

a)

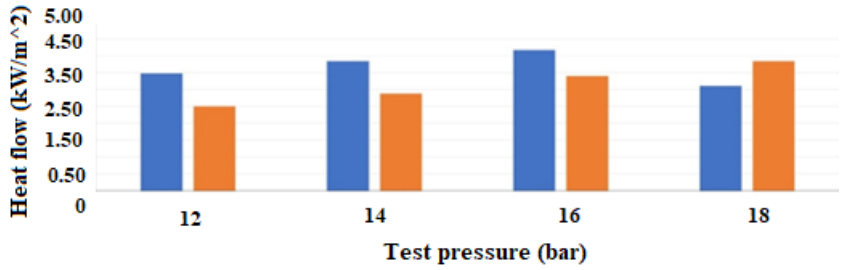

b)

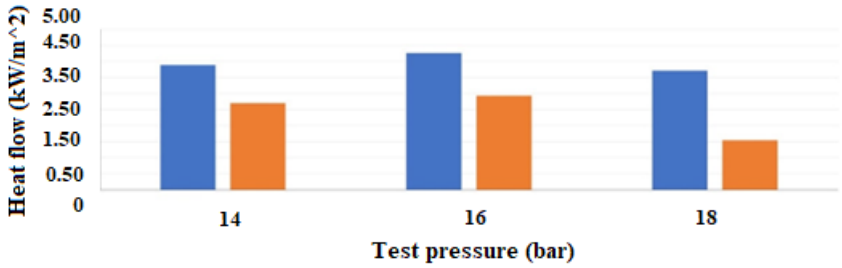

c)

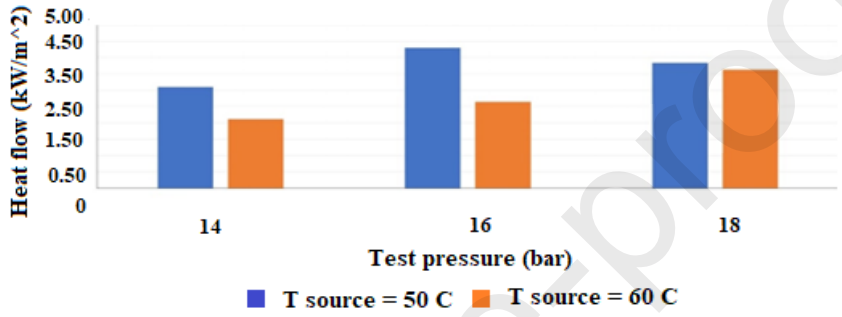

d)

Figure 9. Variation of the heat flow for LMTD 12 to 15 °C. Mass fractions of CO_2 (X_{CO2}) dissolved in acetone a) 22% b) 25% c) 28% and d) 31%.

Lastly, figure 10 shows a trend of increase in heat flow if the test pressure increases from 12 to 18 bar, with increments of 2 bar, for a mass fraction of CO_2 dissolved in acetone between 25 and 31%. In this case the highest value of heat flow corresponds to 5.1 kW×m^{-2}, determined at a temperature in the heating water at the inlet of the desorber of 60ºC and a mass fraction of 31% CO_2 in the CO2/acetone mixture.

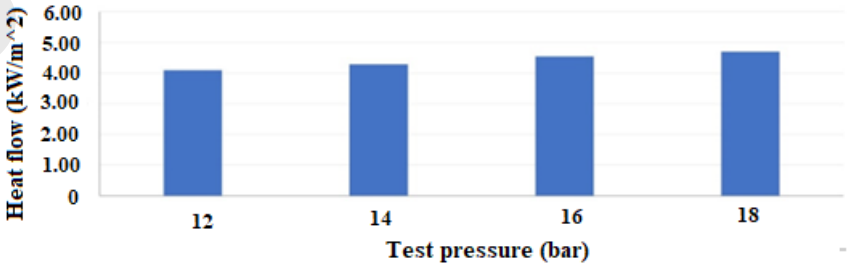

a)

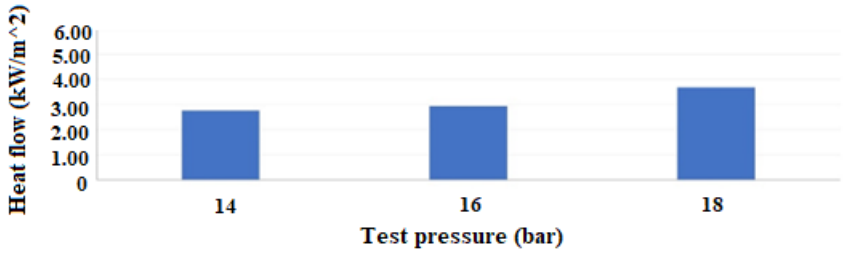

b)

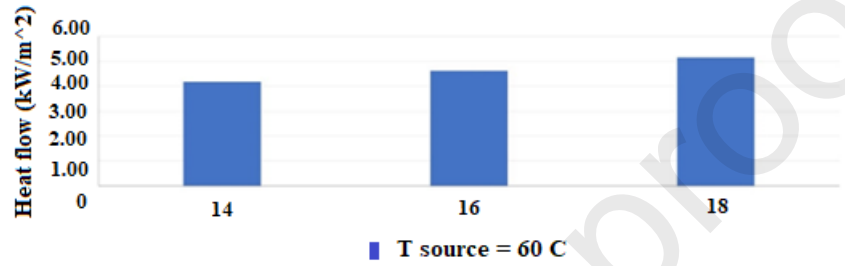

c)

Figure 10. Variation of the heat flow for LMTD 15 to 20 °C. Mass fractions of CO_2 (X_{CO2}) dissolved in acetone a) 25% b) 28% and c) 31%.

3.4 Desorption mass flow

It has been determined that the values of the m_{des} comply with the same general trends as the q" determined for a LMTD between 5 to 20ºC, a heating water temperature at the T_{source} between 40 and 60ºC, a mass fractions of CO_2 dissolved in acetone of 22, 25, 28 and 31%, and a test pressure between 10 to 18 bar. In this sense, the results of m_{des} for a LMTD between 5 and 12ºC, show that at the rate of an increase in mass fraction of CO_2 dissolved in acetone from 22 to 31%, with increases of 2.5% approximately, the mass flow of desorption reaches a higher value of 0.0035, 0.0049, 0.0050 and 0.0050 kg × $s^{-1}.m^{-2}$, at a higher pressure in the test of 14, 14, 16, 18 bar, respectively. Moreover, a trend of reduction in the values of m_{des} is shown when the temperature of the heating water increases from 40 to 60ºC. This trend is repeated for temperatures between 50 and 60ºC for a LMTD between 12 and 15ºC, however, this trend changes for some values to 18 bar of test pressure, where the solution enters the exchanger in subcooling. On the other hand, it was found that for a LMTD between 12 and 15ºC and a heating water temperature of 40ºC, no valid values of m_{des} were determined because the generation of a desorption process of the CO_2/acetone mixture in the central channel of the exchanger, also, for a LMTD between 15 and 20ºC m_{des} results were determined only for a heating water temperature at the desorber input equal to 60ºC. Overall, the values of m_{des} increase their value when the mass fraction of CO_2 dissolved in acetone also does from 22 to 31% delivering an average trend of 10%. In this way, the highest values determined in m_{des} are in a range between 0.004 to 0.005 kg×$s^{-1}m^{-2}$, these values are determined at a T_{source} of 60ºC.

3.5 Development of an empirical correlation in the desorption process for the heat transfer coefficient of the CO_2/acetone mixture in a plate heat exchanger

To validate the experimental data obtained in this work, an empirical correlation has been determined to calculate the value of the heat transfer coefficient of the solution. With the use of this correlation, the deviations determined between the experimental data and the correlation of the heat transfer coefficient of the CO_2/acetone mixture have been determined. At this point it is worth mentioning a previous work where the properties of the CO_2/acetone mixture have been determined and deviation values have been obtained between experimental data of liquid-vapor equilibrium and those obtained by means of a mathematical model. The reviewed bibliography that has served as the basis for this item, development and validation of the developed correlation is presented in Appendix C.

3.6 Model validation study

The work of Oronel et al., [36] and Táboas et al., [38], who used the same plate heat exchanger with NH_3 mixtures for the study of the desorption process in absorption cooling systems, has been reviewed and their results were compared with those of this work, where, Oronel et al., [36] conducted a study of heat transfer in the desorption of ammonia-based working fluids in the plate heat exchanger for absorption cooling systems, and Táboas et al., carried out an study of the forced boiling process of the NH_3/H_20 mixture in the plate heat exchanger for absorption cooling. In this sense, table 6 compiles the operating conditions used in these works, in terms of pressure, temperature and concentration, as well as the intervals of variation of the heat transfer coefficient, heat flow and desorption mass flow.

Table 6. Operating conditions and results in heat transfer parameters

Parameter/Reference	**Present work**	**Oronel et al.** [36]	**Táboas et al.** [38]
$\dot{m}_s$ (kg×m^{-2}s^{-1})	50 to 60	50 to 100	70 to 140
T (˚C)	40 to 60	80 to 120	60 to 90
P (Bar)	10 to 18	5.1	7 to 15
x	0.22 to 0.31	0.50 to 0.54	0.33 to 0.65
h_s (kW×m^{2}K^{-1})	0.10 to 0.50	1.50 to 5.20	5 to 15
q'' (kW×m^{-2})	1.50 to 5.20	5 to 20	20 to 70
$\dot{m}_{da}$ (kg× m^{-2}s^{-1} x10^{-3})	2 to 5	2 to 6	1.5 to 4.5

q_{med}	0.02 to 0.16	0.02 to 0.14	0.02 to 0.22

This work has determinate a value of the heat transfer coefficients (hs) in order of 0.5 $kW \times m^{-2}K^{-1}$ with a q_{med} of 0.16, to T_{source} of 40ºC, a P_{test} of 12 bar, a LMTD between 5 and 12ºC and an X_{CO2} between 22 and 25%. The values of h_s decrease if T_{source} increases to 50 and 60ºC, P_{test} up to 18 bar, a *LMTD* of 20ºC and an X_{CO2} up to 31%, it has been determined that the solution can be found in subcooling at a pressure of 18 bar.

Table 7 shows a summary of the transport properties of working fluids used in research comparable to those obtained from the CO_2/acetone mixture:

Table 7. Comparison of the transport properties of the working fluids with the CO_2/acetone mixture

Parameter/Reference	**Present Study. K. Liu & Kiran; Li et al.**	**Conde-Petite**	**Libotean et al.,**	**Cuenca et al.,**
Working Fluid	CO_2/acetone	NH_3/H_2O	$NH_3/LiNO_3$ (1)	$NH_3/(LiNO_3+H_2O)$ (2)
$\boldsymbol{\mu}$ (mPa×s^{-1})	0.21	0.74	9.53 (1)	3.32 (2)
$\boldsymbol{k_{transf}}$ (W×m^{-1}K^{-1})	0.075	0.560	0.348 (1)	0.353 (2)
$\boldsymbol{\rho}$ (kg×m^{-3})	803.90	850	1166.6 (1)	1117.1 (2)
$\boldsymbol{Qv}$ (kJ×kg^{-1})	288.8	1074	1074	(1)-(2)

[18][22][56][13][14]

The values of h_s of the CO_2/acetone solution obtained in this work are lower than those obtained by the aforementioned studies. The heat transfer coefficient is in the order of average magnitude of 1:30 with respect to Táboas et al., and 1:10 for Oronel et al. The heat flow in the plate heat exchanger is in the average order of magnitude of 1:20 with respect to Táboas et al., and 1:5 for Oronel et al. Regarding the obtained mean vapour quality in the exchanger, this is a value that coincides with the order of magnitude of values of these two other works.

Furthermore, bibliographic review of transport properties of the mixtures NH_3/H_2O, $NH_3/LiNO_3$ and $NH_3/(LiNO_3+H_2O)$ has been carried out with those obtained in the present work for the CO_2/acetone mixture. This comparison was intended to obtain a reference of the behaviour of its refrigerants to the same operating conditions in terms of pressure, temperature, and composition. In this way, table 7 compiles the values of different transport properties for mixtures NH_3/H_2O, $NH_3/LiNO_3$, $NH_3/(LiNO_3+H_2O)$ and CO_2/acetone.

The viscosity of the CO_2/acetone mixture has a ratio of 1:3 with respect to the mixture NH_3/H_2O and a ratio for $NH_3/LiNO_3$ and $NH_3/(LiNO_3+H_2O)$ of 1:45 and 1:15, respectively. In this sense, the lower numerical value of the viscosity of the CO_2/acetone mixture with respect to the compared mixtures indicates more favourable conditions for heat transfer within the plate heat exchanger channel. Even more, regarding the thermal conductivity of the CO_2/acetone mixture, it is shown to have a much lower value with respect to the mixtures NH_3/H_2O, $NH_3/LiNO_3$ and $NH_3/(LiNO_3+H_2O)$. On the other hand, a ratio of the thermal conductivity of the CO_2/acetone mixture of 1:8 to the mixture NH_3/H_2O and approximately 1:6 is determined for $NH_3/LiNO_3$ and $NH_3/(LiNO_3+H_2\ O)$. Although, viscosity favours heat transfer, thermal conductivity is a determining factor for the desorption process. This contributes to lower heat transfer coefficient and heat flow in the heat exchanger for the CO_2/acetone mixture compared to the other mixtures used in the comparison. Lastly, the density values of the CO_2/acetone mixture determined are of the same order of magnitude as those presented for mixtures NH_3/H_2O, $NH_3/LiNO_3$ and $NH_3/(LiNO_3+H_2O)$. On the other hand, the latent heat of vaporization of CO_2 is low compared to NH_3, defining a reduction ratio of approximately 1:4.

3.7 Uncertainty analysis

A standard combined Type B uncertainty criterion was used using partial derivatives in the calculation formulas to determine the calculated thermodynamic parameters. This is shown applied in an example case of calculation developed in appendix D.

5 Conclusions

Regarding the start-up of the experimental equipment, it was defined that an experimental test is made up of two stages: i) stage of stabilization of test conditions and ii) measurement and storage of data obtained in stationary regime. The duration of each stage was 30 minutes on average.

The highest determined value of h_s is 0.52 $kW\times m^{-2}K^{-1}$, which is found at a test pressure of 12 bar, a LMTD between 5 and 12ºC and a temperature in the heating water at the inlet of the desorber of 40ºC. Lastly, the range of values of h_s determined for all the experiences carried out is between 0.10 and 0.52 $kW\times m^{-2}K^{-1}$. The heat flow decreases its value when at the same pressure in the desorber the temperature of the heating water increases from 40 to 60ºC, a LMTD greater than 12ºC generates an increase in heat transfer up to an order of 5 $kW\times m^{-2}K^{-1}$, and the given heat flow range is in the values between 1.5 and 5.1 $kW\times m^{-2}$. A vapor quality value of 16% was achieved in the desorption process of the CO_2/acetone mixture, which is a value like that obtained under similar conditions for Ammonia mixtures. The average range in which m_{des} is defined for the tests

carried out is between 0.002 and 0.005 $kg \times s^{-1}$. In this way, regarding the results obtained from the mass flow of desorption it was determined that the most influential variables are the test pressure and heating water temperature at the inlet of the desorber.

There were no problems with fluid filtration or mixing during the tests on the plate heat exchangers or in the connection pipes of the test bench (approximately 6 months). Regarding the long-term use of acetone, it is recommended to verify that the plate joint in heat exchangers is made of FPM material (gaskets normally used in high-temperature and/or aggressive chemical services).

Furthermore, by comparing the determined values of the heat transfer coefficient of the mixture CO_2/acetone and heat flow with those obtained in literature for mixtures NH_3/H_2O and $NH_3/LiNO_3$, it is concluded that these responds to an order of smaller magnitude due to the thermal conductivity and latent heat of vaporization of the refrigerant. It was found that, although the viscosity of the CO_2/acetone mixture favors heat transfer, the thermal conductivity is a determining factor for the desorption process. This contributes to the lower heat transfer coefficient and heat flux in the exchanger for the CO_2/acetone mixture compared to other mixtures used under similar conditions.

Regarding the criteria studied for nucleated and convective boiling, it is concluded that the experimental case studies of the desorption process of the CO_2/acetone mixture in a plate heat exchanger are in nucleated boiling mode, and lastly, from the results obtained from h_s of the CO_2/acetone mixture, the coefficients of an empirical correlation have been adjusted to determine the heat transfer coefficient of the CO_2/acetone solution in a wider range than that studied in this work.

With respect to the range of values obtained for the heat transfer coefficient of the CO_2/acetone mixture, it is observed that these are relatively low values for a heat pump application and can be better focused on a refrigeration cycle such as in the automotive industry or in the heating of a hybrid water heating system for domestic use.

Consistent with the above idea, in terms of practical application and use of the results in the context of energy conversion and management, future work is planned where the resorber component is studied and subsequently the complete compression/resorption heat pump cycle using the mixture CO_2/acetone. However, this requires compressors that work with CO_2, that is, at a pressure above 60 bar. On the other hand, the development of wet compressor technology that has been under development in recent decades is also expected.

The impact on the energy market and the environment of the application of this technology can be analysed once it is achieved that the cycle components can adapt to the thermal conditions analysed in the cycle operating conditions.

6 Acknowledgments

This study is part of an R&D project funded by the Ministry of Economy, Industry and Competitiveness of Spain (DPI2015-71306-R). Paúl Dávila thanks the Rovira i Virgili University for awarding the Martí-Franqués 2016 (2016PMF-PIPF-26) to obtain a PhD.

7 References

[1] J. T. Gao, Z. Y. Xu, and R. Z. Wang, "An air-source hybrid absorption-compression heat pump with large temperature lift," *Appl. Energy*, vol. 291, p. 116810, Jun. 2021, doi: 10.1016/J.APENERGY.2021.116810.

[2] L. Jiang, R. Q. Wang, X. Tao, and A. P. Roskilly, "A hybrid resorption-compression heat transformer for energy storage and upgrade with a large temperature lift," *Appl. Energy*, vol. 280, p. 115910, Dec. 2020, doi: 10.1016/J.APENERGY.2020.115910.

[3] C. Liu, Y. Jiang, W. Han, and Q. Kang, "A high-temperature hybrid absorption-compression heat pump for waste heat recovery," *Energy Convers. Manag.*, vol. 172, pp. 391–401, Sep. 2018, doi: 10.1016/J.ENCONMAN.2018.07.027.

[4] J. Zhang, H. H. Zhang, Y. L. He, and W. Q. Tao, "A comprehensive review on advances and applications of industrial heat pumps based on the practices in China," *Appl. Energy*, vol. 178, pp. 800–825, Sep. 2016, doi: 10.1016/J.APENERGY.2016.06.049.

[5] M. Wang, C. Deng, Y. Wang, and X. Feng, "Exergoeconomic performance comparison, selection and integration of industrial heat pumps for low grade waste heat recovery," *Energy Convers. Manag.*, vol. 207, p. 112532, Mar. 2020, doi: 10.1016/J.ENCONMAN.2020.112532.

[6] C. Arpagaus, F. Bless, M. Uhlmann, J. Schiffmann, and S. S. Bertsch, "High temperature heat pumps: Market overview, state of the art, research status, refrigerants, and application potentials," *Energy*, vol. 152, pp. 985–1010, Jun. 2018, doi: 10.1016/J.ENERGY.2018.03.166.

[7] M. U. Ahrens *et al.*, "Identification of Existing Challenges and Future Trends for the Utilization of Ammonia-Water Absorption–Compression Heat Pumps at High Temperature Operation," *Appl. Sci.*, vol. 11, no. 10, 2021, doi: 10.3390/app11104635.

[8] L. L. Vasiliev, D. A. Mishkinis, A. A. Antukh, A. G. Kulakov, and L. L. Vasiliev, "Resorption heat pump," *Appl. Therm. Eng.*, vol. 24, no. 13, pp. 1893–1903, Sep. 2004, doi: 10.1016/J.APPLTHERMALENG.2003.12.018.

[9] V. Mučić, "Two media resorption compression heat pump with solution circuit," *J. Heat Recover. Syst.*, vol. 5, no. 1, pp. 27–31, Jan. 1985, doi: 10.1016/0198-7593(85)90118-3.

[10] R. J. B. Moreira-da-Silva, D. Salavera, and A. Coronas, "Modelling of CO2/acetone fluid mixture thermodynamic properties for compression/resorption refrigeration systems," *{IOP} Conf. Ser. Mater. Sci. Eng.*, vol. 595, no. 1, p. 12030, Sep. 2019, doi: 10.1088/1757-899x/595/1/012030.

[11] G. A. Longo, "Heat transfer and pressure drop during HFC refrigerant saturated vapour condensation inside a brazed plate heat exchanger," *Int. J. Heat Mass Transf.*, vol. 53, no. 5–6, pp. 1079–1087, Feb. 2010, doi: 10.1016/J.IJHEATMASSTRANSFER.2009.11.003.

[12] C. W. Jung, S. S. An, and Y. T. Kang, "Thermal performance estimation of ammonia-

water plate bubble absorbers for compression/absorption hybrid heat pump application," *Energy*, vol. 75, pp. 371–378, Oct. 2014, doi: 10.1016/J.ENERGY.2014.07.086.

[13] S. Libotean, A. Martín, D. Salavera, M. Valles, X. Esteve, and A. Coronas, "Densities, viscosities, and heat capacities of ammonia + lithium nitrate and ammonia + lithium nitrate + water solutions between (293.15 and 353.15) K," *J. Chem. Eng. Data*, vol. 53, no. 10, pp. 2383–2388, 2008, doi: 10.1021/je8003035.

[14] Y. Cuenca, D. Salavera, A. Vernet, A. S. Teja, and M. Vallès, "Thermal conductivity of ammonia + lithium nitrate and ammonia + lithium nitrate + water solutions over a wide range of concentrations and temperatures," *Int. J. Refrig.*, vol. 38, no. 1, pp. 333–340, Feb. 2014, doi: 10.1016/J.IJREFRIG.2013.08.010.

[15] B. Markmann *et al.*, "Experimental results of an absorption-compression heat pump using the working fluid ammonia/water for heat recovery in industrial processes," *Int. J. Refrig.*, vol. 99, pp. 59–68, Mar. 2019, doi: 10.1016/J.IJREFRIG.2018.10.010.

[16] L. Cheng, G. Xia, and Q. Li, "CO2 Evaporation Process Modeling: Fundamentals and Engineering Applications," *Heat Transf. Eng.*, vol. 43, no. 8–10, pp. 658–678, May 2022, doi: 10.1080/01457632.2021.1905297.

[17] G. Mozurkewich, M. L. Greenfield, W. F. Schneider, D. C. Zietlow, and J. J. Meyer, "Simulated performance and cofluid dependence of a CO2-cofluid refrigeration cycle with wet compression," *Int. J. Refrig.*, vol. 25, no. 8, pp. 1123–1136, Dec. 2002, doi: 10.1016/S0140-7007(02)00004-X.

[18] K. Liu and E. Kiran, "Viscosity, Density and Excess Volume of Acetone + Carbon Dioxide Mixtures at High Pressures," *Ind. Eng. Chem. Res.*, vol. 46, no. 16, pp. 5453–5462, Aug. 2007, doi: 10.1021/ie070274w.

[19] J. A. Young, "Acetone," *J. Chem. Educ.*, vol. 78, no. 9, p. 1175, Sep. 2001, doi: 10.1021/ed078p1175.

[20] E. Groll and H. Kruse, "Kompressionskältemaschine mit lösungskreislauf für umweltverträgliche kältemittel," *KK Die Kälte und Klimatechnik*, vol. 45, pp. 206–218, 1992.

[21] H. O. Spauschus and U. Hesse, "Reduced pressure carbon dioxide-based refrigeration system," US6112547A, 2000.

[22] H. Li, Ø. Wilhelmsen, Y. Lv, W. Wang, and J. Yan, "Viscosities, thermal conductivities and diffusion coefficients of CO2 mixtures: Review of experimental data and theoretical models," *Int. J. Greenh. Gas Control*, vol. 5, no. 5, pp. 1119–1139, Sep. 2011, doi: 10.1016/J.IJGGC.2011.07.009.

[23] K. Li, W. Wu, J. Wu, H. Liang, and H. Zhang, "Experiments on vapour-liquid equilibrium of CO2-ionic liquid under flow conditions and influence on its refrigeration cycle," *Appl. Therm. Eng.*, vol. 180, p. 115865, Nov. 2020, doi: 10.1016/J.APPLTHERMALENG.2020.115865.

[24] Z. Jin, T. M. Eikevik, P. Nekså, A. Hafner, and R. Wang, "Annual energy performance of R744 and R410A heat pumping systems," *Appl. Therm. Eng.*, vol. 117, pp. 568–576, May 2017, doi: 10.1016/J.APPLTHERMALENG.2017.02.072.

[25] Y. Zhao, B. Yu, B. Wang, S. Zhang, and Y. Xiao, "Heat integration and optimization of direct-fired supercritical CO2 power cycle coupled to coal gasification process," *Appl.*

Therm. Eng., vol. 130, pp. 1022–1032, Feb. 2018, doi: 10.1016/J.APPLTHERMALENG.2017.11.069.

[26] Z. Sun *et al.*, "Experimental study on CO2/R32 blends in a water-to-water heat pump system," *Appl. Therm. Eng.*, vol. 162, p. 114303, Nov. 2019, doi: 10.1016/J.APPLTHERMALENG.2019.114303.

[27] C. M. Hsieh and J. Vrabec, "Vapor–liquid equilibrium measurements of the binary mixtures CO2 + acetone and CO2 + pentanones," *J. Supercrit. Fluids*, vol. 100, pp. 160–166, May 2015, doi: 10.1016/J.SUPFLU.2015.02.003.

[28] J. Wu, Q. Pan, and G. L. Rempel, "Pressure−Density−Temperature Behavior of CO2/Acetone, CO2/Toluene, and CO2/Monochlorobenzene Mixtures in the Near-Critical Region," *J. Chem. Eng. Data*, vol. 49, no. 4, pp. 976–979, Jul. 2004, doi: 10.1021/je0342771.

[29] G. E. Ramírez-Ramos, Y. Zgar, D. Salavera, Y. Coulier, K. Ballerat-Busserolles, and A. Coronas, "Vapor-liquid equilibrium, liquid density and excess enthalpy of the carbon dioxide+acetone mixture: Experimental measurements and correlations," *Fluid Phase Equilib.*, vol. 532, p. 112915, Mar. 2021, doi: 10.1016/J.FLUID.2020.112915.

[30] X. Tao, E. Dahlgren, M. Leichsenring, and C. A. Infante Ferreira, "NH3 condensation in a plate heat exchanger: Experimental investigation on flow patterns, heat transfer and frictional pressure drop," *Int. J. Heat Mass Transf.*, vol. 151, p. 119374, Apr. 2020, doi: 10.1016/J.IJHEATMASSTRANSFER.2020.119374.

[31] J. C. Jiménez-García and W. Rivera, "Parametric analysis on the experimental performance of an ammonia/water absorption cooling system built with plate heat exchangers," *Appl. Therm. Eng.*, vol. 148, pp. 87–95, Feb. 2019, doi: 10.1016/J.APPLTHERMALENG.2018.11.040.

[32] J. Huang, T. J. Sheer, and M. Bailey-McEwan, "Performance of Plate Heat Exchangers Used as Refrigerant Liquid-Overfeed Evaporators." pp. 183–191, Aug. 08, 2010, doi: 10.1115/IHTC14-22095.

[33] T. S. Khan, M. S. Khan, M. C. Chyu, and Z. H. Ayub, "Experimental investigation of evaporation heat transfer and pressure drop of ammonia in a 60° chevron plate heat exchanger," *Int. J. Refrig.*, vol. 35, no. 2, pp. 336–348, Mar. 2012, doi: 10.1016/J.IJREFRIG.2011.10.018.

[34] D. Sterner and B. Sunden, "Performance of Plate Heat Exchangers for Evaporation of Ammonia," *Heat Transf. Eng.*, vol. 27, no. 5, pp. 45–55, Jun. 2006, doi: 10.1080/01457630600559611.

[35] L. C. M. Itard and C. H. M. Machielsen, "Considerations when modelling compression/resorption heat pumps," *Int. J. Refrig.*, vol. 17, no. 7, pp. 453–460, Jan. 1994, doi: 10.1016/0140-7007(94)90005-1.

[36] C. Oronel, C. Amaris, M. Bourouis, and M. Vallès, "Heat and mass transfer in a bubble plate absorber with NH3/LiNO3 and NH3/(LiNO3 + H2O) mixtures," *Int. J. Therm. Sci.*, vol. 63, pp. 105–114, Jan. 2013, doi: 10.1016/J.IJTHERMALSCI.2012.07.007.

[37] C. Amaris, M. Bourouis, M. Vallès, D. Salavera, and A. Coronas, "Thermophysical properties and heat and mass transfer of new working fluids in plate heat exchangers for absorption refrigeration systems," *Heat Transf. Eng.*, vol. 36, no. 4, pp. 388–395, 2015,

doi: 10.1080/01457632.2014.923983.

[38] F. Táboas, M. Vallès, M. Bourouis, and A. Coronas, "Assessment of boiling heat transfer and pressure drop correlations of ammonia/water mixture in a plate heat exchanger," *Int. J. Refrig.*, vol. 35, no. 3, pp. 633–644, May 2012, doi: 10.1016/J.IJREFRIG.2011.10.003.

[39] X. Tao and C. A. Infante Ferreira, "Heat transfer and frictional pressure drop during condensation in plate heat exchangers: Assessment of correlations and a new method," *Int. J. Heat Mass Transf.*, vol. 135, pp. 996–1012, Jun. 2019, doi: 10.1016/J.IJHEATMASSTRANSFER.2019.01.132.

[40] A. Zendehboudi, Z. Ye, A. Hafner, T. Andresen, and G. Skaugen, "Heat transfer and pressure drop of supercritical CO2 in brazed plate heat exchangers of the tri-partite gas cooler," *Int. J. Heat Mass Transf.*, vol. 178, p. 121641, Oct. 2021, doi: 10.1016/J.IJHEATMASSTRANSFER.2021.121641.

[41] J. Rigola, N. Ablanque, C. D. Pérez-Segarra, and A. Oliva, "Numerical simulation and experimental validation of internal heat exchanger influence on CO2 trans-critical cycle performance," *Int. J. Refrig.*, vol. 33, no. 4, pp. 664–674, Jun. 2010, doi: 10.1016/J.IJREFRIG.2009.12.030.

[42] N. García-Hernando, J. A. Almendros-Ibáñez, G. Ruiz, and M. De Vega, "On the pressure drop in Plate Heat Exchangers used as desorbers in absorption chillers," *Energy Convers. Manag.*, vol. 52, no. 2, pp. 1520–1525, Feb. 2011, doi: 10.1016/J.ENCONMAN.2010.10.020.

[43] M. Pitarch, E. Navarro-Peris, J. Gonzalvez, and J. M. Corberan, "Analysis and optimisation of different two-stage transcritical carbon dioxide cycles for heating applications," *Int. J. Refrig.*, vol. 70, pp. 235–242, Oct. 2016, doi: 10.1016/J.IJREFRIG.2015.08.013.

[44] N. Hayes, A. Jokar, and Z. H. Ayub, "Study of carbon dioxide condensation in chevron plate exchangers; heat transfer analysis," *Int. J. Heat Mass Transf.*, vol. 54, no. 5–6, pp. 1121–1131, Feb. 2011, doi: 10.1016/J.IJHEATMASSTRANSFER.2010.11.010.

[45] A. Pérez Sánchez, R. M. Segura Silva, J. R. Montalván Viart, E. Ranero González, and E. J. Pérez Sánchez, "Evaluación térmico-hidráulica de un intercambiador de calor de tubo y coraza para el calentamiento de acetona," *Nexo Rev. Científica*, vol. 34, no. 04, pp. 1075–1097, Oct. 2021, doi: 10.5377/nexo.v34i04.12629.

[46] ASTRALPOOL, "Intercambiador de Placas," *ASTRALPOOL*, 2019. https://asset.productmarketingcloud.com/api/assetstorage/3096_6e50fcef-1df0-421e-938b-4d04e119b207.

[47] E. A. Groll, "Current Status of Absorption/Compression Cycle Technology," *ASHRAE Trans.*, vol. 103, pp. 361–374, 1997, [Online]. Available: https://www.proquest.com/scholarly-journals/current-status-absorption-compression-cycle/docview/2547671775/se-2.

[48] M. Hultén and T. Berntsson, "The compression/absorption heat pump cycle—conceptual design improvements and comparisons with the compression cycle," *Int. J. Refrig.*, vol. 25, no. 4, pp. 487–497, Jun. 2002, doi: 10.1016/S0140-7007(02)00014-2.

[49] S. Klein and G. Nellis, *Thermodynamics*, 1st ed. Madison: Cambridge University Press, 2011.

[50] P. Dávila, "Bomba de calor de compresión/resorción con CO2/acetona: modelización termodinámica del ciclo y estudio teórico-experimental del proceso de desorción en un intercambiador de calor de placas," Universitat Rovira i Virgili, 2020.

[51] M. Berdasco, M. Vallès, and A. Coronas, "Thermodynamic analysis of an ammonia/water absorption–resorption refrigeration system," *Int. J. Refrig.*, vol. 103, pp. 51–60, Jul. 2019, doi: 10.1016/J.IJREFRIG.2019.03.023.

[52] T. S. Khan, M. S. Khan, M. C. Chyu, and Z. H. Ayub, "Experimental investigation of single phase convective heat transfer coefficient in a corrugated plate heat exchanger for multiple plate configurations," *Appl. Therm. Eng.*, vol. 30, no. 8–9, pp. 1058–1065, Jun. 2010, doi: 10.1016/J.APPLTHERMALENG.2010.01.021.

[53] Y. Y. Hsieh and T. F. Lin, "Evaporation heat transfer and pressure drop of refrigerant R-410A flow in a vertical plate heat exchanger," *J. Heat Transfer*, vol. 125, no. 5, pp. 852–857, 2003, doi: 10.1115/1.1518498.

[54] J. T. Cieśliński, A. Fiuk, K. Typiński, and B. Siemieńczuk, "Heat transfer in plate heat exchanger channels: Experimental validation of selected correlation equations," *Arch. Thermodyn.*, vol. 37, no. 3, pp. 19–29, 2016, doi: 10.1515/aoter-2016-0017.

[55] K. E. Herold, R. Radermacher, and S. A. Klein, *Absorption Chillers and Heat Pumps*, Second. New York: CRC Press, 2016.

[56] M. Conde-Petite, "Thermophysical Properties of NH3+H2O Mixtures for the Industrial Design of Absorpion Refrigeration Equipment. Formulation for Industrial Use," Zurich, 2006. [Online]. Available: http://www.mrc-eng.com/Downloads/NH3&H2O Props English.pdf.

[57] S. G. Kandlikar, "A model for correlating flow boiling heat transfer in augmented tubes and compact evaporators," *J. Heat Transfer*, vol. 113, no. 4, pp. 966–972, 1991, doi: 10.1115/1.2911229.

[58] A. E. Bergles, "Forced - convection surface boiling heat transfer and burnout in tubes of small diameter," Massachusetts Institute of Technology, 1962.

[59] V. D. Donowski and S. G. Kandlikar, "Correlating evaporation heat transfer coefficient of refrigerant R-134a in a heat plate exchanger," in *Engineering Foundation Conference on Pool and Flow Boiling*, 2000, pp. 1–18.

4 APPENDIX

Appendix A

Instrumentation and control for the experimental study of the desorption process of the CO_2/acetone mixture in a plate heat exchanger

The solution tank is a 26-liter stainless steel tank who has an internal coil through which a fluid other than that contained inside the tank can circulate. In the present study, this coil is connected to the cooling equipment (CE), glycol water is used at 35% by weight as a fluid for the cooling of the CO_2 / acetone mixture located in the solution tank. The solution tank has several input and output connections and two auxiliary connections for the external connection of the internal coil. Furthermore, a Coriolis type flowmeter is available to measure the density and mass flow that is driven by the pump rotor, that corresponds to an Emerson/CMF025 mode l, has a flow/density measurement accuracy of ± 0.10%, 0.5 $kg \times m^{-3}$, respectively, supports a maximum and minimum flow rate of 0.005 and 0.020 $kg \times s^{-1}$, a maximum operating pressure of 30 bar and an operating temperature range between -20 and 60ºC. The pump selected for the experimental equipment is a gear pump made of stainless steel. This pump corresponds to the manufacturer Tuthill, model DGS.57EEET2NN+SM423, has an operating temperature range between -20/50 ºC, a maximum operating pressure of 24 bar, maximum pressure ratio of 2.5 and a minimum and maximum operating flow of 5 and 30 $l \times h^{-1}$, respectively. On the other hand, for the measurement of the temperature of the solution currents, cooling and heating water, 4-wire Pt 100 thermo-resistors were used, with a maximum temperature limit of 250ºC, and an accuracy of ± 0.10 ºC, where all probes have been previously calibrated using thermal bath #1, in a calibration interval between 20 and 80ºC, in this way, calibration lines were established for each of the sensors to ensure a repeatability of ± 0.05ºC. The pressure measurement used pressure transmitters located at the inlet and outlet of each component of the experimental equipment for the study of the desorption process of the CO_2/acetone mixture as shown in Figure 3. Pressure sensors have an upper operating limit of 30 bar, the output range is 4-20 mA, and the accuracy of these sensors is 0.1% of the working pressure of the equipment. These pressure sensors have been calibrated in an interval between 2 and 20 bar, where calibration lines were established for each of the sensors to ensure a repeatability of ± 0.01 bar. Lastly, the data acquisition system corresponds to the Keysight brand, model Agilent 34970A, who measures voltages, direct and alternating currents, sensor resistors to 2 and 4 wires, frequencies, and period. It has two accommodations for data acquisition cards with 40 channels each.

Appendix B

Loading of the CO_2/acetone mixture in the experimental equipment, tuning and determination of stationary conditions

Once all the components have been assembled in the respective order (Figure 3). It is secured that there are no leaks in the solution circuit of the experimental equipment with a tightness test performed with compressed air that entered the installation up to a pressure of 5 bar. Leaks in the equipment have been reduced to a maximum of 0.1 bar per test day. The correct operation of the solution impulsion pump, heating and cooling thermal baths is verified.

The control of the quantity of each pure fluid (CO_2 and acetone) is carried out by difference in weights of their respective containers considering their density. Acetone is in liquid phase at atmospheric pressure and average temperature of 20ºC, it has been initially deposited to achieve a progressive absorption at the entry of CO_2 into the mixing load circuit. On the other hand, for the CO_2 a commercial cylinder at 57 bar of internal pressure was used, so the outlet to the loading circuit is made through a pressure regulating valve. Once both components have been introduced, the mixture circulates through the mixing charge circuit initiated in the tank, cooling in the capacitor and returning to the starting point.

Furthermore, each experimental test involves two stages: i) stage of stabilization of test conditions and ii) measurement and storage of data obtained in stationary regime. The duration of each stage was 30 minutes on average and the criteria considered for stationary regime are the following:

- The density of the solution measured in the Coriolis type flowmeter is considered constant when the measured value does not exceed a fluctuation value ± 0.5 $kg \times m^{-3}$ in the measurement for a minimum period of 30 minutes.
- The temperature of the solution measured on the corresponding temperature sensor is considered stable, where the precision value of the sensor of ± 0.10ºC was assumed as the maximum tolerance.

The experiments carried out were grouped into several series of trials. A series of tests was considered when the experimental facility was loaded with a defined amount of CO_2 and was absorbed by acetone in the solution tank. In this way, with the load carried out, a set of tests determined by the variation of the operating conditions in the experimental installation was defined.

Appendix C

Regarding plate heat exchangers Longo, [11] studied the effect of saturation temperature in function of pressure for the mass flow and heat transfer properties of HFC refrigerants on brazed plate heat exchangers. In this way, it was found that the heat transfer coefficients displayed a weak sensitivity to the temperature of saturation in function of pressure but regarding the mass flux and the fluid properties of the refrigerant showed a great sensitivity, and even more a single trend of an equivalent of the Reynolds number between 1600-1700 was found to be a critical value in the transition of gravity controlled and forced convection condensation on the working fluids [11]. García-Hernando et al., analysed the pressure drop on the desorption of ammonia-water and lithium bromide – water (LiBr-H_2O) mixtures on plate heat exchangers, where in the case of NH_3 the desorption temperature difference was found to be negligible compared regarding the pressure drops. However, in the case of the LiBr-H_2O solution there was found desorption temperature changes as high as 30°C and pressures drops of 20kPa. Therefore, the authors concluded that the key element on absorption chiller of plate heat exchangers that operates with LiBr-H_2O, is the pressure drops and hence the initial boiling temperature [42].

In the research of Cheng et al., [16] it has been analysed the modelling and mechanisms of evaporation heat transfer of CO_2 on macro-channels and micro-channels, showing different characteristics for the evaporation heat transfer and two phase flow at saturation temperatures ranging from 0 to 25C, where CO_2 delivers a much higher evaporation heat transfer than other refrigerants such as the R134a and ammonia. In this way, at low/moderate vapour qualities near the dry out of CO_2 and relative lower qualities than conventional refrigerants, the evaporation heat transfer has a dominance on nucleate boiling. [16]

Kandlikar, [57] suggested that heat exchangers, which serve as compact evaporators, can be treated similarly for analysis as augmented smooth tube exchangers [57]. Bergles, concluded that the nucleation of a hemispherical bubble occurs when the temperature at the liquid interface reaches the minimum temperature required for boiling, where, as the heat flow increases, the vapour quality decreases, the nucleated boiling mode predominates, and since the wall overheating required to activate, a bubble is reached at a lower fluid temperature [58]. Furthermore, in convective boiling the heat transfer coefficient is influenced by the ratio of the density of the liquid to vapour density (ρ_l/ρ_v) for a defined vapor quality r, a higher ratio of results in a higher volume of steam and a higher speed of the two-phase mixture. In this way, according to the criteria set out in the work of Donowski & Kandlikar, [59] the tests carried out on the process of desorption of the CO_2/acetone mixture in the central channel of the plate heat exchanger occur in nucleated boiling mode [59].

Furthermore, an empirical correlation for the prediction of the heat transfer coefficient of the CO_2/acetone (h_s) solution is proposed based on the work of Donowski & Kandlikar [59], who displayed a predictive correlation for the evaporative heat transfer coefficient of the refrigerant R-134a in plate heat exchanger. These authors enunciated two modes of boiling: nucleated and convective dominant and made a proposal for combined boiling that relates both effects. The equations proposed in the aforementioned work for nucleated and convective boiling modes are presented below [59]. Equation (1) shows the correlation that determines the dominant boiling effect, equation (2) the dominant convective boiling effect, and equation (3) the correlation that combines the effect of both boiling modes, where, a boiling flow can be separated into a different

nucleated boiling term, by applying a direct heat at a nucleation sight, also, a moving fluid can be characterized as a heat transfer problem by a convective boiling term.

$$h_{ND} = 0.6683 * Co^{-0.2} * (1 - q_{med})^{0.8} * h_l * E_{CB} + 1058 * Bo^{0.7} * (1 - q_{med})^{0.8} * F_{fl} * h_l * E_{NB} \quad (19)$$

$$h_{CD} = 1.1360 * Co^{-0.9} * (1 - q_{med})^{0.8} * h_l * E_{CB} + 667.2 * Bo^{0.7} * (1 - q_{med})^{0.8} * F_{fl} * h_l * E_{NB} \quad (20)$$

$$h_{NC} = [2.31 * Co^{-0.3} * E_{CB} + 667.3 * Bo^{2.8} * F_{fl} * E_{NB}] * (1 - q_{med})^{0} * h_l \quad (21)$$

Where:

h_{ND} – Heat transfer efficiency with dominant nucleated boiling effect

h_{CD} – Heat transfer efficiency with dominant convective boiling effect

h_{NC} – Heat transfer efficiency with combined boiling effect

Co – Convective number

Bo – Boiling number.

h_{LG} – Specific vaporization enthalpy

F_{fl} – Characteristic friction of the fluid.

In this way, for stainless steel surfaces Kandlikar, suggests that this fluid-dependent parameter is equal to 1 for all fluids. Factors E_{CB} and E_{NB} are enhancement factors that apply to the convective boiling contribution and nucleated boiling contribution, which its values are 0.512 and 0.338 respectively [57]. On the other hand, in the case of the CO_2/acetone mixture, the experimentally determined values of *hs* have been taken and the coefficients of the equation proposed by Donowski & Kandlikar [59]. The equation involving the combined boiling mode (nucleated and convective) has been taken and the expression shown in equation (4) has been obtained.

$$h_{s\_corr} = (0.206 \quad (22)$$

$$* Co^{2.}$$
$$+ 81$$

$$* Bo^{1.}$$

$$- q_{me}$$
$$* h_l$$

In this way, for the adjustment of the coefficients of the proposed correlation, 50 experimental tests of the desorption process of the CO_2/acetone mixture have been used, where table 8 presents in detail the maximum, mean and minimum deviation between experimental values and determined by the empirical correlation for h_s.

Table C 1. Deviations determined between experimental data and by correlation of the heat transfer coefficient of the CO2/acetone mixture.

Mass fraction of CO_2 in the mixture (%)	Minimum deviation (%)	Value in kW×m^{-2}K^{-1}	Mean deviation. (%)	Value in kW×m^{-2}K^{-1}	Maximum deviation (%)	Value in kW×m^{-2}K^{-1}
22	0.2	0.01	7.5	0.025	20.5	0.047
25	0.2	0.01	18.5	0.045	35.9	0.124
28	0.3	0.02	13.1	0.034	12.8	0.046

31	0.07	0.001	15.1	0.035	20.1	0.055

This adjustment has shown a mean deviation of 13.3%, a better fit is obtained between the experimental data and calculated by the proposed correlation in a mass fraction between 28 and 31%. The maximum deviation value of 35.9% is given when the mass fraction of CO_2 in the CO2/acetone mixture is 25%, this value is 0.045 $kW \times m^{-2}K^{-1}$. In this way, there has been obtained that the correlation generates an average deviation of more than 20% only in 12% of the total of experimental cases.

From the comparison between experimental data and determined by correlation of h_s, an average minimum, mean and maximum deviation of 0.2, 13.5 and 22.3%, respectively, was determined.

Appendix D

Calculation and determination of uncertenty

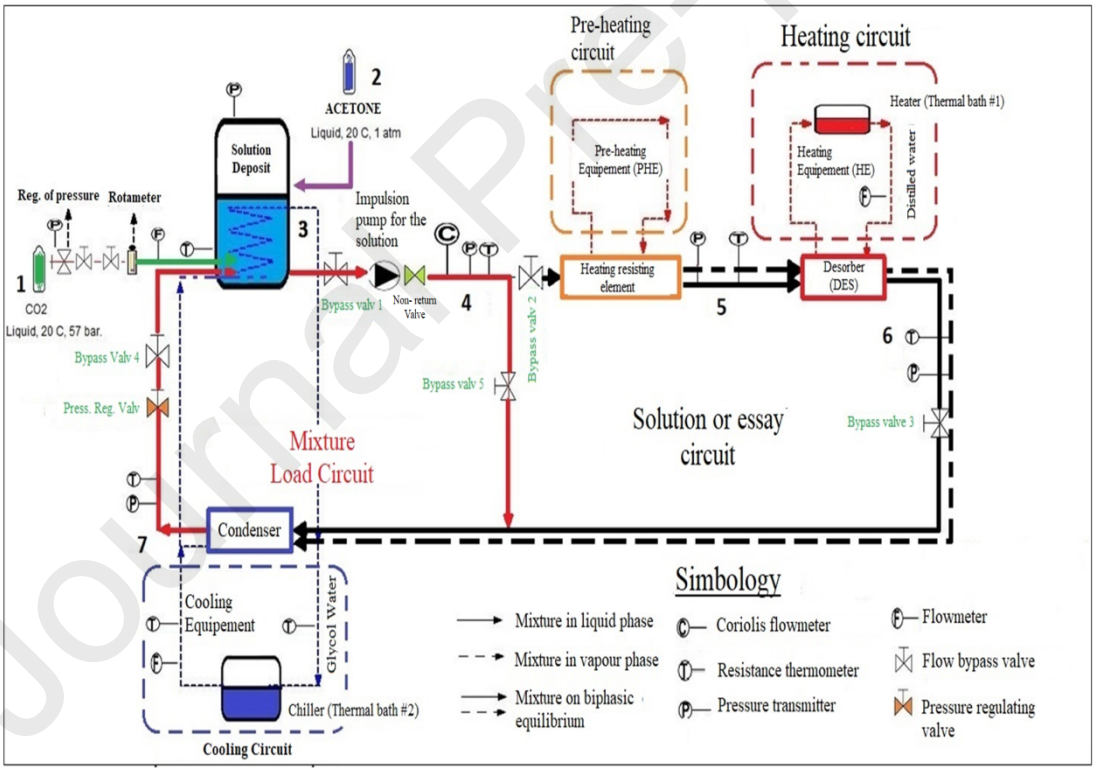

Figure D. 1. Installation scheme

Experimental data:

Test pressure: $P_{[4]}$ = 12.26 bar; pressure measured at Coriolis flow sensor

$P_{[5]}$ = 12.20 bar; pressure measured at desorbent inlet

$P_{[6]}$ = 12.04 bar; pressure measured at desorptive outlet

$\dot{m}_{sol}$= 0.0057 [kg×s^{-1}]; mass flow measured on the Coriolis flow sensor

ρ_{sol} = 830.9600 [kg×m^{-3}]; density measured on the Coriolis flow sensor

$T_{[4]}$ = 18.44 [°C]; temp. From the solution measured in the Coriolis flow sensor

$T_{[5]}$= 20.14 [°C]; temp. From the solution to the desorbing inlet

$T_{[6]}$= 40.50 [°C]; temp. From the solution to the desorption output

$\dot{m}_{ftc}$= 0.0065 [kg×s^{-1}]; Mass Flow of Heating Thermal Fluid

T_{in_ftc}= 48.48 [°C]; temp. at inlet of heating thermal fluid

T_{out_ftc}= 42.53 [°C]; temp. at outlet of heating thermal fluid

Uncertainty of CO_2 concentration

Table D. 1. Uncertainty of CO_2 concentration

Temperature						
Xi	**xi**	**Units**	**Prob. Distribution**	**u(xi)**	**Ci**	**u(yi)**
Repeatability	20.14	ºC	normal	0.051	1	0.003
Calibration	0.11	ºC	rectangular	0.064	1	0.004
Resolution	0.10	ºC	normal	0.050	1	0.003
					$u^2(x)$	**0.009**
					u(x)	**0.096**
Density						
Xi	**xi**	**Units**	**Prob. Distribution**	**u(xi)**	**Ci**	**u(yi)**
Repeatability	830.96	kg×m^{-3}	normal	0.074	1	0.005
Resolution	0.50	kg×m^{-3}	rectangular	0.144	1	0.021
Calibration	0.10	kg×m^{-3}	normal	0.050	1	0.003
					$u^2(x)$	0.029

					u(x)	0.170
Solution concentration						
Xi	**xi**	**Units**	**Prob. Distribution**	**u(xi)**	**Ci**	**u(yi)**
Temperature	20.13	ºC	normal	0.096	0.01496	2.069E-06
Density	830.96	$kg \times m^{-3}$	normal	0.170	0.01029	3.043E-06
					$u^2(x)$	5.113E-06
					u(x)	0.0023

Uncertainty of the enthalpy of the solution at the entrance of the disorber

Table D. 2. Uncertainty in the calculation of ideal enthalpies of pure fluids

CO_2						
Temperature						
Xi	**xi**	**Units**	**Prob. Distribution**	**u(xi)**	**Ci**	**u(yi)**
Repeatability	20.14	ºC	normal	0.051	1	0.003
Calibration	0.11	ºC	rectangular	0.064	1	0.004
Resolution	0.10	ºC	normal	0.050	1	0.003
					$u^2(x)$	0.009
					u(x)	0.096
Pure CO_2 Enthalpy	168.80	$kJ \times kg^{-1}$	normal	0.096	0.462	0.044
Acetone						

Temperature						
Xi	**xi**	**Units**	**Prob. Distribution**	**u(xi)**	**Ci**	**u(yi)**
Repeatability	0.00	ºC	normal	0.000	1	0.000
Calibration	0.11	ºC	rectangular	0.064	1	0.004
Resolution	0.10	ºC	normal	0.050	1	0.003
					$u^2(x)$	0.007
					u(x)	0.081
Pure Acetone Enthalpy	291.90	$kJ \times kg^{-1}$	normal	0.096	0.982	0.094

Table D. 3. Uncertainty in the calculation of the ideal enthalpy of the mixture

Liquid Phase						
Xi	**xi**	**Units**	**Prob. Distribution**	**u(xi)**	**Ci**	**u(yi)**
Concentration	0,25	$kJ \times kg^{-1}$	normal	0,002	1,000	0,000
Temperature	20,14	ºC	normal	0,096	1,456	0,020
					$u^2(x)$	0,020
					u(x)	0,140
Vapour Phase						
Xi	**xi**	**Units**	**Prob. Distribution**	**u(xi)**	**Ci**	**u(yi)**
Concentration	0,25	$kJ \times kg^{-1}$	normal	0,002	1,000	0,000
Temperature	20,14	ºC	normal	0,096	0,597	0,003

					$u^2(x)$	0,003
					u(x)	0,057

Table D. 4. Uncertainty in the calculation of work pressure

Xi	xi	Units	Prob. Distribution	u(xi)	Ci	u(yi)
Repeatability	12,20	bar	normal	0,0073	1	5,31E-05
Calibration	0.01	bar	rectangular	0,0058	1	3,33E-05
Resolution	0.11	bar	normal	0,0500	1	0,0025
			normal		**$u^2(x)$**	0,0025
					u(x)	**0,050**

Table D. 5. Uncertainty in the calculation of the enthalpy of mixture formation

Liquid Phase

Xi	xi	Units	Prob. Distribution	u(xi)	Ci	u(yi)
Concentration	0,25	$kg \times kg^{-1}$	normal	0,002	1,000	0,000
Temperature	20,14	˚C	normal	0,096	8,122	0,610
Pressure	12.20	bar	normal	0,051	-11,070	0,317
					$u^2(x)$	0,927
					u(x)	0,963

Vapour Phase						
Xi	**xi**	**Units**	**Prob. Distribution**	**u(xi)**	**Ci**	**u(yi)**
Concentration	0,250	kg×kg^{-1}	normal	0,002	1,000	0,000
Temperature	20,14	˚C	normal	0,096	-0,842	0,007
Pressure	12,20	bar	normal	0,051	15,960	0,659
					u^2(x)	0,665
					u(x)	0,816

Table D. 6. Uncertainty in the calculation of the enthalpy of mixing at each stage

Liquid Phase						
Xi	**xi**	**Units**	**Prob. Distribution**	**u(xi)**	**Ci**	**u(yi)**
Concentration	0,25	kg×kg^{-1}	normal	0,002	1,000	0,000
Temperature	20,14	˚C	normal	0,096	1,183	0,013
Pressure	12,20	bar	normal	0,051	3,513	0,032
					u^2(x)	0,045
					u(x)	0,212

Vapour Phase						
Xi	**xi**	**Units**	**Prob. Distribution**	**u(xi)**	**Ci**	**u(yi)**

Concentration	0,25	kg×kg^{-1}	normal	0,002	1,000	0,000
Temperature	20,14	˚C	normal	0,096	0,980	0,009
Pressure	12,20	bar	normal	0,051	-1,219	0,004
					u^2(x)	0,013
					u(x)	0,113

Table D. 7. Uncertainty of the overall enthalpy of the solution at the input of the desorber

Xi	**xi**	**Units**	**Prob. Distribution**	**u(xi)**	**Ci**	**u(yi)**
Concentration	0,25	kg×kg^{-1}	normal	0,002	568	1,650
Temperature	20,14	ºC	normal	0,096	3,512	0,114
Pressure	12,20	bar	normal	0,051	-6,371	0,105
					u^2(x)	1,869
					u(x)	1,367

Uncertainty of the enthalpy of the solution at the exit of the desorber

Table D. 8. Uncertainty in the calculation of ideal enthalpies of pure fluids

CO_2						
Temperature						
Xi	**xi**	**Units**	**Prob. Distribution**	**u(xi)**	**Ci**	**u(yi)**
Repeatability	40,50	ºC	normal	0,022	1	0,000
Calibration	0,11	ºC	rectangular	0,064	1	0,004

Resolution	0,10	ºC	normal	0,050	1	0,003
					$u^2(x)$	0,007
					u(x)	0,084
Pure CO_2 Enthalpy	179,00	kJ/kg	normal	0,084	0,545	0,046

Acetone						
Temperature						
Xi	**xi**	**Units**	**Prob. Distribution**	**u(xi)**	**Ci**	**u(yi)**
Repeatability	40,50	ºC	normal	0,000	1	0,000
Calibration	0,11	ºC	rectangular	0,064	1	0,004
Resolution	0,10	ºC	normal	0,050	1	0,003
					$u^2(x)$	0,007
					u(x)	0,081
Pure Acetone Enthalpy	313,50	kJ×kg^{-1}	normal	0,084	1,148	0,096

Table D. 9. Uncertainty in the calculation of the ideal enthalpy of the mixture

Liquid Phase						
Xi	**xi**	**Units**	**Prob. Distribution**	**u(xi)**	**Ci**	**u(yi)**
Concentration	0,25	kg×kg^{-1}	normal	0,002	1,000	0,000
Temperature	40,50	ºC	normal	0,084	1,443	0,015
					$u^2(x)$	0,015

					u(x)	0,122
Vapour Phase						
Xi	**xi**	**Units**	**Prob. Distribution**	**u(xi)**	**Ci**	**u(yi)**
Concentration	0,25	kg×kg^{-1}	normal	0,002	1,000	0,000
Temperature	40,50	ºC	normal	0,084	0,848	0,005
					u^2(x)	0,005
					u(x)	0,072

Table D. 10. Uncertainty in the calculation of work pressure

Xi	**xi**	**Units**	**Prob. Distribution**	**u(xi)**	**Ci**	**u(yi)**
Repeatability	12,04	bar	normal	0,0080	1	6,39E-05
Calibration	0,01	bar	rectangular	0,0058	1	3,33E-05
Resolution	0,12	bar	normal	0,0500	1	0,0025
					u^2(x)	0,0025
					u(x)	0,050

Table D. 11. Uncertainty in the calculation of the enthalpy of mixture formation

Liquid Phase						
Xi	**xi**	**Units**	**Prob. Distribution**	**u(xi)**	**Ci**	**u(yi)**
Concentration	0,25	kg×kg^{-1}	normal	0,002	1,000	0,000

Temperature	40,50	ºC	normal	0,084	7,717	0,425
Pressure	12,04	bar	normal	0,051	-10,490	0,286
					$u^2(x)$	0,711
					u(x)	0,843

Vapour Phase						
Xi	**xi**	**Units**	**Prob. Distribution**	**u(xi)**	**Ci**	**u(yi)**
Concentration	0,25	$kg \times kg^{-1}$	normal	0,002	1,000	0,000
Temperature	40,50	ºC	normal	0,084	-0,132	0,000
Pressure	12,04	bar	normal	0,051	13,700	0,487
					$u^2(x)$	0,487
					u(x)	0,698

Table D. 12. Uncertainty in the calculation of the enthalpy of mixing at each stage

Liquid Phase						
Xi	**xi**	**Units**	**Prob. Distribution**	**u(xi)**	**Ci**	**u(yi)**
Concentration	0,25	$kg \times kg^{-1}$	normal	0,002	1,000	0,000
Temperature	40,50	ºC	normal	0,084	1,638	0,019
Pressure	12,04	bar	normal	0,051	2,386	0,015
					$u^2(x)$	0,034
					u(x)	0,184

Vapour Phase						
Xi	**xi**	**Units**	**Prob. Distribution**	**u(xi)**	**Ci**	**u(yi)**
Concentration	0,25	kg×kg^{-1}	normal	0,002	1,000	0,000
Temperature	40,50	ºC	normal	0,084	0,980	0,007
Pressure	12,04	bar	normal	0,051	-1,324	0,005
					u^2(x)	0,011
					u(x)	0,107

Table D. 13. Uncertainty of the overall enthalpy of the solution at the exit of the desorber

Xi	**xi**	**Units**	**Prob. Distribution**	**u(xi)**	**Ci**	**u(yi)**
Concentration	0,25	kg×kg^{-1}	normal	0,002	537,200	1,208
Temperature	40,50	ºC	normal	0,084	2,903	0,060
Pressure	12,04	bar	normal	0,051	-4,209	0,046
					u^2(x)	1,314
					u(x)	1,146

Heat uncertainty of the heating on the solution side

Table D. 14. Heat uncertainty of the heating on the solution side

Mass Flow						
Xi	**xi**	**Units**	**Prob. Distribution**	**u(xi)**	**Ci**	**u(yi)**
Repeatability	0,0057	$kg \times s^{-1}$	normal	5,246E-06	1	2,753E-11
Calibration	0,0006	$kg \times s^{-1}$	rectangular	8,018E-06	1	6,430E-11
Resolution	0,1000	$kg \times s^{-1}$	normal	1,388E-05	1	1,929E-10
					$u^2(x)$	2,847E-10
					u(x)	1,687E-05
Heat (Q)						
Xi	**xi**	**Units**	**Prob. Distribution**	**u(xi)**	**Ci**	**u(yi)**
Mass Flow	0,0057	$kg \times s^{-1}$	normal	1,687E-05	64,500	1,184E-06
Desorber enthalpy inlet	-213,20	$kJ \times kg^{-1}$	normal	1,369	-0,006	6,129E-05
Desorber enthalpy outlet	-148,70	$kJ \times kg^{-1}$	normal	1,146	0,006	4,295E-05
					$u^2(x)$	1,054 E-04
					u(x)	0,0103

Heat uncertainty on the heating thermal fluid side

Table D. 15. Heat Uncertainty on the Heating Thermal Fluid Side

Mass Flow

Xi	xi	Units	Prob. Distribution	u(xi)	Ci	u(yi)
Repeatability	0,0065	$kg \times s^{-1}$	normal	3,74E-05	1	1,41E-09
Calibration	0,0007	$kg \times s^{-1}$	rectangular	8,01E-06	1	6,43E-11
Resolution	0,1000	$kg \times s^{-1}$	normal	1,38E-05	1	1,93E-10
					$u^2(x)$	**1,66E-09**
					u(x)	**4,08E-05**

Temperature at the inlet of the heating thermal fluid

Xi	xi	Units	Prob. Distribution	u(xi)	Ci	u(yi)
Repeatability	48,48	°C	normal	0,0063	1	0,000
Resolution	0,10	°C	rectangular	0,0289	1	0,001
Calibration	0,20	°C	normal	0,1250	1	0,016
					$u^2(x)$	**0,016**
					u(x)	**0,128**

Temperature at the outlet of the heating thermal fluid

Xi	xi	Units	Prob. Distribution	u(xi)	Ci	u(yi)
Repeatability	42,53	°C	normal	0,0305	1	0,001
Resolution	0,10	°C	rectangular	0,0289	1	0,001
Calibration	0,20	°C	normal	0,1000	1	0,010
					$u^2(x)$	**0,012**
					u(x)	**0,108**

Heat (Q)						
Xi	**xi**	**Units**	**Prob. Distribution**	**u(xi)**	**Ci**	**u(yi)**
Mass flow (m)	0,0065	$kg \times s^{-1}$	normal	4,08E-05	-24,886	1,0298E-06
T_{outlet}	42,52	°C	normal	0,108	0,0272	8,765E-06
T_{inlet}	48,48	°C	normal	0,128	-0,0272	1,229E-05
Specific Heat (Cp)	4,18	$kJ \times kg^{-1} \times K^{-1}$	rectangular	0,001	-0,0388	5,038E-10
					$u^2(x)$	**2,208E-05**
					u(x)	**0,0046**

Declaration of interests

☐ The authors declare that they have no known competing financial interests or personal relationships that could have appeared to influence the work reported in this paper.

☒The authors declare the following financial interests/personal relationships which may be considered as potential competing interests:

- Coronas, Alberto
- Bruno, Joan Carles
- Barba, M. Isabel
- Berdasco, Miguel
- Salavera, Daniel
- Larrechi, M. Soledad
- Valles, Manél